THE UNIVERSITY OF MICHIGAN

INDUSTRY PROGRAM OF THE COLLEGE OF ENGINEERING

STUDY OF POSITIVE TAU MESON DECAYS IN A PROPANE BUBBLE CHAMBER

Theodore Francis Zipf

January, 1958

IP- 269

Doctoral Committee:

Assistant Professor Martin L. Perl, Co-Chairman
Professor Donald A. Glaser, Co-Chairman
Professor Wayne E. Hazen
Associate Professor Maxwell O. Reade
Professor George E. Uhlenbeck

ACKNOWLEDGMENTS

The author wishes to express his gratitude to Professors M. L. Perl and D. A. Glaser who provided friendly advice and guidance whenever it was needed or requested.

The research was supported in part by the United States Atomic Energy Commission.

TABLE OF CONTENTS

LIST OF FIGURES

LIST OF TABLES

CHAPTER I

INTRODUCTION

1.1 Survey of the Heavy Mesons

In 1949 Brown et al.[1] observed, in a photographic emulsion exposed to the cosmic radiation, a particle whose mass was intermediate between that of the π^- meson and that of the proton. This particle came to rest in the emulsion and then decayed into three charged particles. Mass measurements showed that the secondary particles were very probably π^- mesons. Since that time particles of similar mass as that of the particle observed by Brown et al. have been observed. These particles not only have exhibited positive and negative values of the electron charge but also have appeared in the neutral charge state. One of the striking properties of these particles is the large number of ways in which they are observed to decay. It has become customary to refer to these particles as K particles or heavy mesons and to further classify them according to their decay scheme. When only one of the secondaries is charged and the remaining one or more secondaries are neutral the particle is represented by the letter K with two subscripts. The first subscript indicates the type of charged secondary and the second subscript indicates the total number of secondaries involved in the decay. In Table I the known decay modes of the positive and neutral heavy mesons and the percentage of the total number of K's represented by a particular decay mode are listed. The K^- decay modes and the relative abundances of these

TABLE I

DECAY MODES OF THE K^+ AND K° PARTICLES AND PER CENT OF TOTAL K PARTICLES THE DECAY MODE REPRESENTS

Species	Decay Mode	Per Cent of Total K's Represented by Decay Mode
$K^+_{\pi 2}$	$\pi^+ + \pi^\circ$	27%
$K^+_{\mu 2}$	$\mu^+ + \nu$	57%
τ^+	$2\pi^+ + \pi^-$	6%
$K^+_{\pi 3}(\tau'^+)$	$2\pi^\circ + \pi^+$	2%
$K^+_{\mu 3}$	$\mu^+ + \pi^\circ + \nu$	4%
$K^+_{e 3}$	$e^+ + \pi^\circ + \nu$	4%
θ°_1	$\pi^+ + \pi^-$	
θ°_2	$\pi^\pm + e^\mp + \nu$ $\pi^\pm + \mu^\mp + \nu$	
τ°	$\pi^+ + \pi^- + \pi^\circ$	

modes are not as well established as are those for the K^+ case.

Until 1954 the K particles which were observed were those which had been produced in the cosmic radiation. Thus, primarily because it is not possible to produce these particles copiously using cosmic ray intensities, extensive studies of the properties of heavy mesons were not feasible. In 1954, however, it became possible, by

using the high energy, high intensity primary particle beams of the Cosmotron, and later the Bevatron, to produce sufficient numbers of these heavy mesons to be able to determine, accurately their elementary properties. It is the purpose of the following paragraphs in this section to review briefly the results of those investigations.

The mass appears, within the limits of experimental error, to be the same for all of the K^+ particles. Two types of experiments are used to determine the mass. In the primary mass type of measurement the beam of charged particles is first momentum selected by means of a magnetic field and then is brought to rest in an absorber. The knowledge of the range and the momentum allows one to assign a value to the mass since for particles of the same charge in the same absorber the range is a function of velocity only. The other type of mass measurement which has been employed extensively is the so-called "secondary mass measurement." This method consists of measuring the kinetic energy of the secondaries and then, employing the known mass of the secondaries, equating the mass of the primary (in energy units) to the sum of the secondary masses (in energy units) plus the sum of the kinetic energies of the secondaries. Since it is very difficult to measure the energy of an uncharged secondary this method is not applicable to the particles which decay via the $K_{\pi 3}(\tau')$, $K_{\mu 3}$, and K_{e3} modes. It is a very important result that the masses obtained by the secondary method agree well with those obtained by the primary method since this tends to rule out the possibility of the primary K meson undergoing an undetected energy transition to a lower state (that of the immediate parent) which then decays according to the observed mode.[2,3] Table II

shows a comparison of recent mass measurements by means of the two methods.[4]

TABLE II

MEASURED MASSES AND STANDARD DEVIATIONS FOR K^+ MESONS FROM PRIMARY AND SECONDARY METHODS

	Primary Mass	Secondary Mass
τ^+	966.6 ± 1.9	966.1 ± 0.7
$K^+_{\mu 2}$	967.2 ± 2.2	964.8 ± 2.8
$K^+_{\pi 2}$	966.7 ± 2.0	964.2 ± 2.0
$K_{\mu 3}$	966. ± 6	---
K_{e3}	963. ± 10	---

The lifetimes of the τ, $K_{\pi 2}$ and $K_{\mu 2}$ have been measured to a high degree of accuracy by Fitch and Motley using counter techniques.[5,6] They obtain the following values for the lifetime:

$$T(\tau) = (1.17^{+0.08}_{-0.07}) \times 10^{-8} \text{ sec.}$$

$$T(K_{\pi 2}) = (1.21^{+0.11}_{-0.10}) \times 10^{-8} \text{ sec.}$$

$$T(K_{\mu 2}) = (1.17^{+0.08}_{-0.07}) \times 10^{-8} \text{ sec.}$$

These values lie well within the experimental errors of the somewhat less accurate emulsion results.[7,8] The lifetimes of the $K_{\mu 3}$ and K_{e3} have been measured only by means of the emulsion technique.[9] The lifetimes so obtained are

$$T(K_{\mu 3}) = (0.88 \pm 0.23) \times 10^{-8} \text{ sec.}$$

$$T(K_{e3}) = (1.44 \pm 0.46) \times 10^{-8} \text{ sec.}$$

which are in agreement with the τ, $K_{\pi 2}$ and $K_{\mu 3}$ lifetimes. Among the neutral K mesons it has been well established recently that there are two types of particles. One of these, the θ°_1, is short lived with a lifetime of [10]

$$T(\theta^\circ_1) = (0.74^{+0.21}_{-0.15}) \times 10^{-10} \text{ sec.}$$

The other, the θ°_2, is long lived with a lifetime of roughly 10^{-8} sec.[11]

At present, the data regarding the scattering and the production of K^+ mesons is rather scant. Thus it is difficult to state whether or not there exists a coorelation between the interactions of the particle and the mode by which it decays.

Thus it might appear that one is led to the tentative conclusion that the K^+ particles should be considered as a single parent particle with several modes of decay. The difficulty in this approach arises when an attempt is made to assign non-classical properties to the parent K particle. For some time it has been assumed that among the set of simultaneous observables unique to a given nuclear particle, are the intrinsic spin and the intrinsic parity (i.e, the behavior of the wave function of the particle under inversion of the space coordinates) of the particle. In other words, it is required that for any transition between states the total angular momentum of the system and the behavior of the wave function of the system under the parity operation remain invariant. Then using the laws of conservation of parity and angular momentum it can be shown that the $K_{\pi 2}$ cannot have either spin zero and odd parity, or spin one and even parity. It can also be shown that the τ cannot have spin zero and even parity but for spin one it can have

either even or odd parity. Thus if the $K_{\pi 2}$ and τ are the same particle then this particle cannot have spin zero. Experimentally no spin effects have been observed for the $K_{\pi 2}$,[12] while several emulsion experiments have indicated that the spin of the τ may be zero and also that the τ does not have spin one and odd parity (denoted by 1-). So from the viewpoint of mass, lifetime, and interaction properties all of the K^+ particles seem to be identical, but if spin and parity are taken into account one finds that, if the spin is zero or one, the particles may not be identical. Furthermore, there appears to be no means, within the framework of present day physics, of explaining this difference if parity is conserved in the decay. This presents a problem, often referred to popularly as the "τ-θ puzzle," which is one of the major difficulties in the understanding of high energy nuclear phenomena.

1.2 Further Consideration of the K Particles and the Aim of the Present Investigation.

The problem which was introduced in the previous section suggests two possible areas of further research. The first, and perhaps most obvious, approach is a more exhaustive experimental study of the K particle properties, while the second requires a careful re-examination of the presently accepted theoretical concepts of contemporary nuclear physics. Clearly, these two types of research are not independent, for the correctness of a proposed theory can only be judged by reference to accurate experimental results, and useful experimentation derives its direction from theoretical conjecture.

A great deal of experimental research remains to be done in the study of the behavior of the secondaries emitted in K meson decay. That

such work can yield information regarding the primary follows from the fact that it is possible to predict the behavior of the secondaries if certain properties of the primary are known. In most cases the information, concerning the primary, which must be known are quantum mechanical parameters. If the laws of conservation of angular momentum and parity are assumed to be valid then the relevant parameters are the spin and the intrinsic parity. The method which is used in decay studies then is to predict the behavior of a given decay mode for different values of the spin and parity. The results of experiment are then compared with these theoretical predictions. The spin and parity which lead to calculated results consistent with experiment are then taken to be the correct values. The τ meson is a particularly good subject for this type of study since it decays into three charged secondaries which, because of their charge, are easily observed. Dalitz[14,15] and Fabri[16] have predicted the energy and angular distributions of the secondaries. All of these calculations have assumed the validity of the law of conservation of parity. Recently several experimenters have examined the energy and angular distributions from large samples of τ mesons decaying from rest in nuclear emulsions.[13,17] The data collected from all of these experiments are compatible with 0- and 2- and several sets have been compatible with 1+. Perhaps the most salient feature about all of these experiments is that none of them, either individually or when combined, give close agreement with any one of the predicted distributions. Thus there is some justification for the existance of a certain amount of doubt as to the correctness of the assumptions used in calculating the theoretical spectrum.. Lee and Yang[18] have examined in detail the validity of the

law of conservation of parity. Although they have not been able to resolve the uncertainties surrounding the nature of the K particles, they have been successful in that they have provided the impetus for experiments whose results contain extremely important physical information. Wu et al.[19,20] and Garwin, Lederman and Weinrich[21] have established that parity is not conserved in those weak interactions (i.e., slow processes) associated with β decay, and the decay of the π and the μ mesons. As yet it has not been ascertained experimentally whether or not this result extends to other weak interactions which do not involve the neutrino. With this in mind Lomon[22] has calculated the π^- energy and angular spectrum for τ decay assuming the non-conservation of parity. He finds some disagreement with the world data for a spin zero τ meson but by adjusting certain constants, which is allowed, he finds that he can obtain fair statistical agreement with a spin two τ meson. It is important to note that Lomon's results depend heavily on the assumption that no experimental bias exists in the world data.

The present investigation was undertaken in an attempt to collect and analyze data on τ meson decay by means of an experimental method which differs somewhat from the photographic emulsion technique which has been used exclusively by previous investigators. In this experiment the τ mesons are brought to rest and then decay in a propane bubble chamber.

Although a detailed discussion of nuclear emulsions is beyond the scope of this work a brief comparison of this technique with bubble chamber methods is of value. In emulsions tracks resulting from a large number of beam pulses are observed in the field of view of the microscope

used for the scanning. The scanner must follow a track of correct blob density to its end and further must identify the decay mode by following each decay product to its end. In the bubble chamber technique, on the other hand, each pulse of the beam is photographed with a stereo camera. The greater range of the secondaries in propane as compared to that in emulsion "enlarges" the decay event to an extent such that the scanning of the bubble chamber photographs may be done either with the naked eye or with low magnification viewers. The two stereo photographs give the scanner views of two spatial orientations of the event and this tends to increase the efficiency with which the events may be identified. In the emulsion technique, the scanner, in most cases, is limited to one orientation of the event, and this condition may give rise to a geometrical bias in this type of experiment. It is one of the purposes of this experiment to ascertain whether or not such a geometrical bias exists in the emulsion data on τ^+ meson decays. A rough estimate of the length of scanning time required for emulsion and bubble chamber experiments, each with the same number of events, shows that the bubble chamber scanning time would be approximately one-third of that required for emulsions. Since the time required to measure and analyze the events is approximately the same for both techniques this factor of three represents the increase in speed of experimentation made possible by the bubble chamber technique.

CHAPTER II

THEORETICAL CONSIDERATIONS IN τ^+ MESON DECAY

2.1 The Kinematics of τ^+ Meson Decay

The effects of the laws of conservation of momentum and energy on the reaction $\tau^+ \rightarrow \pi^+ + \pi^+ + \pi^-$ will now be considered. The positive and negative pions will be assumed to have the same mass.

First consider a three body decay in the laboratory coordinate system for the case in which the center of mass of the three particle system is in motion. At any instant in time the positions of the three particles may be represented by the vectors $\vec{r}_1$, $\vec{r}_2$, and $\vec{r}_3$, where the origin of the coordinate system is taken to be an arbitrary point in space. In this problem all three particles have the same mass and the particles whose positions are given by $\vec{r}_1$ and $\vec{r}_2$ are the identical pions. The momenta conjugate to $\vec{r}_1$, $\vec{r}_2$, and $\vec{r}_3$ are the individual particle momenta $\vec{p}_1$, $\vec{p}_2$, and $\vec{p}_3$. The kinematics of τ decay can be given for this completely general case in terms of the coordinates and momenta introduced above, but for investigations, such as this, in which the spin angular momentum of the decaying particle is to be determined the coordinate system which is chosen is that system in which the decaying particle is at rest, that is, the center of mass system. In the following the center of mass system will be used exclusively and the vertex of the event will be taken as the origin. In this system the law of conservation of momentum provides the constraint that the vector sum of the momenta of the decay products must equal zero. This requires that the momentum vectors of the three pions lie in the same plane. Thus the

problem now requires the knowledge of only two momenta and it is therefore convenient to define a new system of variables.

Since particles 1 and 2 are identical no generality is lost if these two momenta are combined to give a single new momentum. The new system of variables defined for the general case of τ^+ decay will consist of three momenta and three space variables. The new momenta will be: $\vec{P}$, which is proportional to the sum of the three pion momenta, $\vec{p}$, which is proportional to the relative momentum of the two like pions, and $\vec{p}'$, which is proportional to the momentum of the odd pion, in this case the π^-, with respect to the center of mass of the system consisting of the two positive pions. The new space variables will be the coordinates conjugate to $\vec{P}$, $\vec{p}$, and $\vec{p}'$, namely $\vec{R}$, $\vec{r}$, and $\vec{r}'$. In particular, these new variables are

$$\vec{P} = \frac{1}{\sqrt{3}} (\vec{p}_1 + \vec{p}_2 + \vec{p}_3)$$

$$\vec{p} = \frac{1}{\sqrt{2}} (\vec{p}_2 - \vec{p}_1) \qquad (2\text{-}1)$$

$$\vec{p}' = \sqrt{\frac{2}{3}} \left[\vec{p}_3 - \frac{1}{2} (\vec{p}_1 + \vec{p}_2) \right]$$

and

$$R = \frac{1}{\sqrt{3}} (\vec{r}_1 + \vec{r}_2 + \vec{r}_3)$$

$$r = \frac{1}{\sqrt{2}} (\vec{r}_2 - \vec{r}_1) \qquad (2\text{-}2)$$

$$r' = \sqrt{\frac{2}{3}} \left[\vec{r}_3 - \frac{1}{2} (\vec{r}_1 + \vec{r}_2) \right]$$

This system of variables was first introduced by Fabri[16] and the transformation from $\vec{r}_1$, $\vec{r}_2$, $\vec{r}_3$ and $\vec{p}_1$, $\vec{p}_2$, $\vec{p}_3$ to $\vec{R}$, $\vec{r}$, $\vec{r}'$ and $\vec{P}$, $\vec{p}$, $\vec{p}'$ is referred to as the "Fabri Transformation". Figure 1 is a momentum diagram

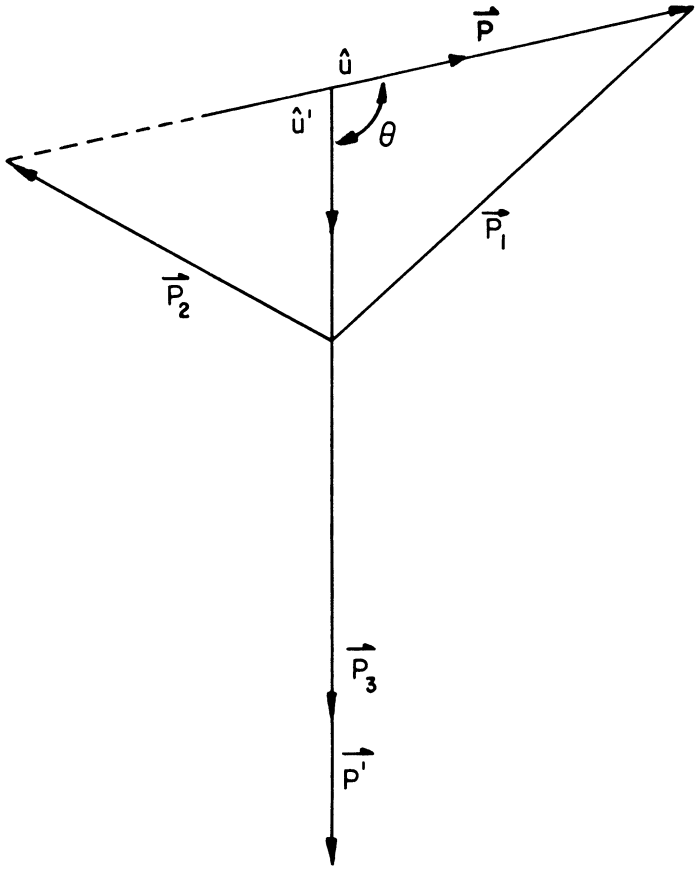

FIGURE 1 Momentum Diagram

showing the quantities introduced above. From (2-1) it follows that the center of mass system is defined by $\vec{P} = 0$. The choice of constant coefficients is such that the total angular momentum in this system is

$$\vec{J} = \vec{j} + \vec{j}' \tag{2-3}$$

where

$$\begin{aligned} \vec{j} &= \vec{r} \times \vec{p} \\ \vec{j}' &= \vec{r}' \times \vec{p}' \end{aligned} \tag{2-4}$$

In later sections it will be found convenient to separate the moduli of the vectors $\vec{p}$ and $\vec{p}'$ from the unit vectors $\hat{u}$ and $\hat{u}'$ which give their direction. From equation (2-1) it follows that

$$\begin{aligned} p^2 &= p_1^2 + p_2^2 - 1/2\, p_3^2 \\ p'^2 &= 3/2\, p_3^2 \\ \cos\theta &= \hat{u} \cdot \hat{u}' = \frac{1}{\sqrt{2}} \frac{(p_1^2 - p_2^2)}{\left[p_3^2(p_1^2 + p_2^2 - 1/2\, p_3^2)\right]^{1/2}} \end{aligned} \tag{2-5}$$

where θ is the angle between $\vec{p}$ and $\vec{p}'$.

The law of conservation of energy can be expressed for the case of τ decay as

$$E_1 + E_2 + E_3 = M = 3m + Q \tag{2-6}$$

where E_i is the total energy of the i^{th} particle, M and m are the rest masses (in energy units) of the τ and π mesons respectively, and Q is the total kinetic energy given to the pions on decay of the τ from rest. For a three body decay in the center of mass system two parameters are sufficient to specify completely the kinematics. Thus all possible kinematical states can be represented in a two dimensional

space. More specifically, it is possible to establish a one to one correspondence between the two parameters which determine the decay configuration and the points of a plane region. The conservation of energy and momentum will limit the allowed area. The conservation of energy requires that the sum of three pion energies be equal to the Q value of the decay, approximately 75 Mev. A geometrical representation of this is provided by the equilateral triangle which has the property that the algebraic sum of the perpendicular distances from the three sides of the triangle to any point interior to the triangle is equal to a constant, the altitude of the triangle. Thus all possible states allowed by the conservation of energy will be represented by points lying in the interior of an equilateral triangle of altitude Q. This triangle has been drawn in Figure 2. The perpendicular distance from a given side of the triangle to a point representing the state will be equal to the kinetic energy of one of the particles appearing in the decay. Using a polar coordinate system, (ρ, φ), with the pole at the geometric center of the triangle and measuring φ from an axis passing through the pole and one of the vertices, the following expressions for the total energies of the particles are obtained

$$\begin{aligned} E_1 &= \frac{M}{3}\left[1 + \rho K \cos\left(\varphi - \frac{2\pi}{3}\right)\right] \\ E_2 &= \frac{M}{3}\left[1 + \rho K \cos\left(\varphi + \frac{2\pi}{3}\right)\right] \\ E_3 &= \frac{M}{3}\left[1 + \rho K \cos \varphi\right] \end{aligned} \qquad (2\text{-}7)$$

where $K = \frac{Q}{M}$. Since $E_i^2 = p_i^2 + m^2$ then p^2, p'^2, and $\cos\theta$ can be written as

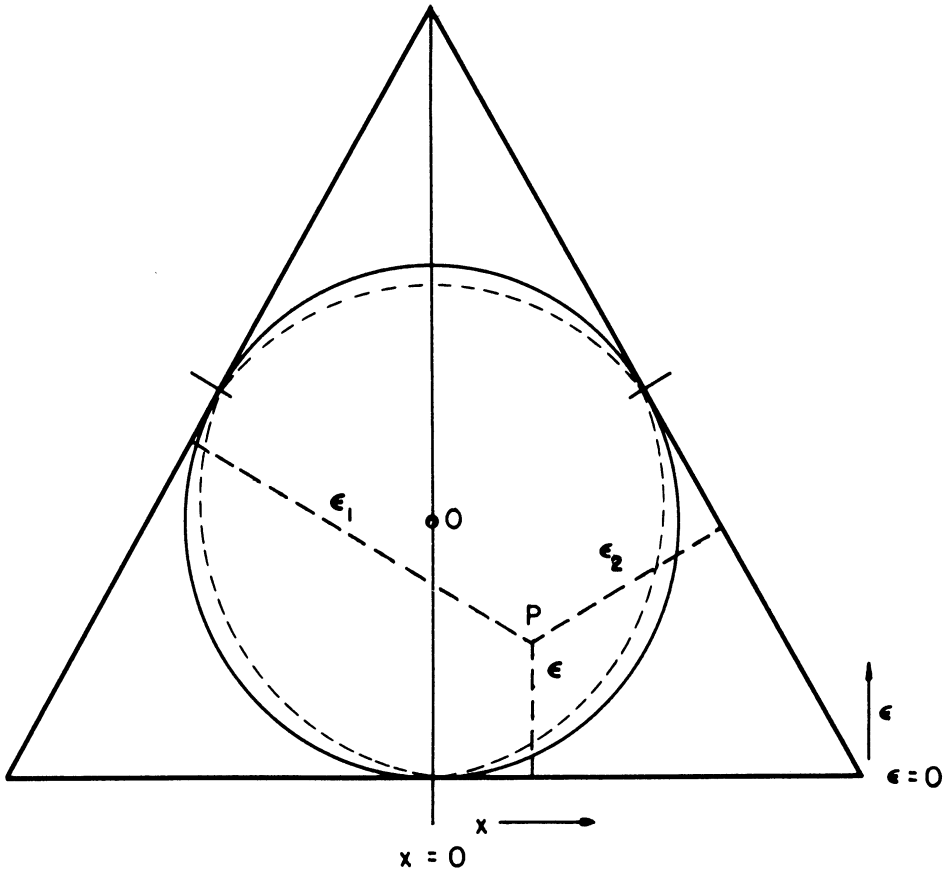

FIGURE 2 Phase Space For Meson Decay

$$p^2 = \frac{M^2}{3} K \left[(1 - \rho \cos \varphi) - \frac{1}{2} K (1 - \rho^2 \sin^2 \varphi)\right]$$

$$p'^2 = \frac{M^2}{3} K (1 + \rho \cos \varphi) \left[1 - \frac{1}{2} K (1 - \rho \cos \varphi)\right] \qquad (2\text{-}8)$$

$$\cos \theta = \frac{\rho \sin \varphi (1 - \frac{1}{2} K \cos \varphi)}{[(1-\rho \cos \varphi) - \frac{1}{2} K(1-\rho^2 \cos^2\varphi)]^{1/2}[(1-\rho \cos \varphi) - \frac{1}{2} K(1-\rho^2 \sin^2\varphi)]^{1/2}}$$

It is clear that all the points contained in the interior of the triangle cannot represent allowed states of the system. For example, the vertices of the triangle are ruled out because this would correspond to one particle receiving all the energy and this, of course, is not compatible with the conservation of momentum. When K is small the non-relativistic energy-momentum relations may be employed and then it can be shown that the maximum energy which any particle can receive in the decay is equal to 2/3 Q. Furthermore, it can be shown that, under this condition, the effect of conservation of momentum is to limit the allowed states to the interior of a circle which is tangent to each side of the triangle at its midpoint as shown in Figure 2. When K is not small, the situation is somewhat more complicated. Using the conservation of momentum and $E_i^2 = p_i^2 + m^2$, where E_i is given in terms of ρ and φ in (2-7), it is possible to show that the allowed region is limited by a cubic of the form

$$\rho^3 + \frac{(1 + \alpha)}{\alpha \cos 3\varphi} \rho^2 - \frac{1}{\alpha \cos 3\varphi} = 0, \qquad (2\text{-}9)$$

where $\alpha = 1/2\ K\ (1 - 1/2\ K)^2 = 0.09$. Note that in the non-relativistic limit $(K \to 0)$(and therefore $\alpha \to 0$) this equation reduces to the equation of a circle. Equation (2-9) is represented by the dotted line in Figure 1, and the non-relativistic region is the solid circle. Reference to this figure shows that the non-relativistic approximation is a rather good one for

this problem. The results obtained when it is not possible to consider K as a small quantity simply restrict the permitted region somewhat, which in turn changes the maximum energy received by any one of the pions from the non-relativistic result of 2/3 Q to approximately 0.96(2/3)Q.

2.2 Comparison of the Spin-Parity Properties of the θ^+ and τ^+

In this section the effects of the laws of conservation of parity and angular momentum on τ^+ meson decay will be considered. The first investigation of these effects was carried out by Dalitz.[14,15] This was followed by the work of Fabri.[16] The presentation given here follows closely the work of these two authors.

Before proceeding with the analysis it is first necessary to make certain definitions. An arbitrary direction in space is taken as the axis of quantization, and this is denoted by the unit vector $\hat{u}_o$. The eigenvalues of the square of the total angular momentum $|\vec{J}|^2$ are $J(J+1)$ and those of $\vec{J} \cdot \hat{u}_o$ are m_J. Similarly $|\vec{J}|^2$ and $|\vec{j}'|^2$ have eigenvalues $\ell(\ell+1)$ and $\ell'(\ell'+1)$ respectively and $\vec{j} \cdot \hat{u}_o$ and $\vec{j}' \cdot \hat{u}_o$ have the eigenvalues m and m'. The final state can be written as a function of p, $\hat{u}$, $\hat{u}'$ and will be an eigenstate of $|\vec{J}|^2$ and $\vec{J} \cdot \hat{u}_o$ relative to the J and m_J corresponding to the spin of the τ^+ and its orientation in space with respect to the axis of quantization.

The law of conservation of angular momentum applied to τ decay requires the total angular momentum of the three pion final state to be equal to the initial spin angular momentum of the τ. The law of conservation of parity states that the behavior of the final state wave function under inversion of coordinates must be the same as that of the initial state wave function under the same operation. This latter rule

can be applied to a hypothetical decay process such as $A \rightarrow B + C + \ldots$ in the following way: assume that the final state can be represented by a wave function which is proportional to the product of the wave functions of the individual particles B, C, etc. It is assumed that these wave functions can be written in such a way as to exhibit a definite symmetry with regard to inversion of the space coordinates. Then the symmetry of the product wave function under spatial inversion is the same as the combination of the individual symmetries under the same operation. It is customary to represent the symmetry by (± 1) depending upon whether or not the wave function changes sign upon inversion. Then the combination of the individual symmetries takes the form $(+1)(-1) = -1$ etc. Thus in the two body decay $A \rightarrow B + C$, if the wave function for A has odd parity and the wave function for B has even parity then the wave function for C must have odd parity. The parity of the individual wave function is the product of the intrinsic parity of the particle and the parity of the state. If the wave function is an eigenfunction of the angular momentum then the parity of an orbital angular momentum state goes as $(-1)^{\ell}$.

As an example of a simple application of the angular momentum and parity conservation rules the case of the θ° meson will be considered. The θ° meson is known to have a decay of the form

$$\theta^\circ \rightarrow \pi^+ + \pi^- \qquad \text{(a)}$$

and may undergo the decay

$$\theta^\circ \rightarrow \pi^\circ + \pi^\circ. \qquad \text{(b)}$$

The π meson has odd intrinsic parity so the final state wave functions for both (a) and (b) contain a term $(-1)^2$ upon inversion, that is, there is no sign change of the final state wave function due to the intrinsic

parity of the π mesons. The θ° has an angular momentum $\vec{J}$ and the conservation of angular momentum requires the final state for (a) and (b) to have an angular momentum equal to that of the initial state. The orbital angular momentum for a two pion system is just $\vec{r} \times \vec{p} = \vec{\ell}$ where $\vec{r}$ is the relative position vector and $\vec{p}$ is the relative momentum. Since the spin of the pion is zero the only angular momentum which can enter into the final state is that arising from an orbital state. Thus the final state will be an eigenstate of $|\vec{\ell}|^2$ and the projection of $\vec{\ell}$ along the axis of quantization, $\vec{\ell} \cdot \hat{u}_o$. Thus the conservation of angular momentum is simply $\vec{J} = \vec{\ell}$. The parity of the final state wave function will then depend upon whether ℓ is even or odd. If the spin of the θ° is odd, then the parity is odd, and, if the spin of the θ° is even, then the θ° has even parity. Process (a) can take on all values of ℓ and thus the knowledge of the existence of (a) yields little information about the spin of the θ°. The existence of process (b), however, would restrict the possible spins of the θ°. This restriction arises from the fact that two neutral pions are identical bosons, which requires that the wave function representing the system formed by the two must not change under the interchange of the two particles. Such a wave function must have a value of ℓ which is even. Thus if the two π° decay mode of the θ° exists then the θ° has even spin and even intrinsic parity.

Next consider the case of the K^+ or θ^+ which decays as $\theta^+ \rightarrow \pi^+ + \pi^\circ$. Here the ℓ of the final state can be odd or even with corresponding parity. Therefore, the θ^+ must have spin-parity combinations of the type: (0+), (1-), (2+), etc.

Finally consider the somewhat more complicated case of τ^+ decay. This particle is known to undergo the decays

$$\tau^+ \rightarrow \pi^+ + \pi^+ + \pi^- \qquad (a')$$

$$\tau^{+\prime} \rightarrow \pi^+ + \pi^\bullet + \pi^\circ \qquad (b')$$

In both (a') and (b') the parity of the final state wave function due to the intrinsic parity of the three pions is $(-1)^3$, or odd. Thus the parity of the final state wave function is $(-1)P'$ where P' is the parity of the final space state. This will depend upon ℓ, which is proportional to the angular momentum of the two π^+ system, and on ℓ', proportional to the orbital state of the π^- with respect to the center of mass of the two π^+ system. The positive pions are identical bosons and the same argument that was applied to $\theta^\circ \rightarrow 2\pi^\circ$, requires that ℓ be even. Thus the parity of the final state depends only upon the wave function with respect to $\hat{u}'$. It follows that if the parity of the τ^+ is odd then P' must be even which requires ℓ' to be even and, conversely, if the parity of the τ^+ is even then P' must be odd and ℓ' odd. Since the orbital angular momentum must satisfy the condition

$$|\ell - \ell'| \leq J \leq \ell + \ell'$$

it is possible to conclude that for a particle of even parity and zero spin there is no allowed three π-meson decay. For, in order to have $J = 0$, ℓ' must be equal to ℓ, but ℓ must be even and therefore ℓ' must be even which leads to a spin zero particle of odd parity. Therefore, the τ^+ must have one of the following spin-parity combinations: (0-), (1+), (1-), (2+), (2-) etc.

Now the original assumption about the nature of the θ^+ and the τ^+ was that they are different decay modes of the same particle and that

particle has a definite parity and further that parity is conserved in both decay modes. For the θ^+ and τ^+ to be a single particle of definite parity with conservation of parity in the decay the τ^+ decay spectrum must indicate a spin-parity combination of (1-), (2+), (3-) etc.

If such a τ^+ decay spectrum is not found then it is necessary to assume that either the θ^+ and τ^+ are different particles, or that they are the same particle but that the particle does not have a definite parity, or that the parity is not conserved in the decay. If the parity is not conserved in the τ^+ decay then it might be possible to find further evidence for this in the τ^+ decay spectrum by itself without regard to the θ^+ - τ^+ relationship. This is discussed in a later section.

2.3 Calculation of the τ^+ Decay Spectrum for Certain Spin-Parity Combinations

The starting point of the detailed theoretical study of τ^+ meson decay is the general quantum mechanical expression for the transition rate. In this case it is written as

$$\frac{d^2R(p',\cos\theta)}{dp'd(\cos\theta)} = \frac{2\pi}{\hbar}\left|M(p',\cos\theta)\right|^2\rho(p',\cos\theta) \qquad (2\text{-}10)$$

where M(p', cos θ) is the matrix element of the transition and ρ(p', cos θ) is the density in phase space. It is in calculating M(p', cos θ) that the physical assumptions of the model are introduced.

M(p', cos θ) is calculated by considering the matrix elements for the production of momenta $\vec{k}$ and $\vec{k}'$, where $\vec{k} = \vec{p}/\hbar$ and $\vec{k}' = \vec{p}'/\hbar$

respectively. Neglecting final state interactions, the wave function for k is proportional to $e^{i\vec{k}'\cdot\vec{r}}$ and that for $\vec{k}'$ is proportional to $e^{i\vec{k}'\cdot\vec{r}'}$. Then the matrix element for the decay of the τ^+ meson in the state J, m_J into the state described by momenta $\vec{k}$ and $\vec{k}'$ is

$$m(\vec{k},\vec{k}')_{Jm_J} = \int d\vec{r}\int d\vec{r}'\, e^{i\vec{k}\cdot\vec{r}}\, e^{i\vec{k}'\cdot\vec{r}'}\, g_{Jm_J}(\vec{r},\vec{r}') \quad (2\text{-}11)$$

Where, in the g_{Jm_J} there appear terms representing the decay interaction and the initial state wave function which have been integrated over the coordinates of the τ meson. Furthermore, the $g_{Jm_J}(\vec{r},\vec{r}')$ in the integral of (2-11) shall be such that not only is angular momentum conserved but also such that if the integral is expanded in powers of the momentum the series will converge. It is assumed that g_{Jm_J} is not explicitly momentum dependent and also that it is rotationally invariant. Then

$$g_{Jm_J}(\vec{r},\vec{r}') = \sum_{l,l'} f(r,r')_{Jll'} \sum_{m,m'} (ll'mm'|ll'Jm_J) \times Y_l^{m*}(\theta,\varphi)\, Y_{l'}^{m'*}(\theta',\varphi') \quad (2\text{-}12)$$

where $f_{Jll'}$ is independent of m_J. Substituting this into equation (2-11) yields

$$m(\vec{k},\vec{k}') = \int d\vec{r}\int d\vec{r}'\, e^{i\vec{k}\cdot\vec{r}}\, e^{i\vec{k}'\cdot\vec{r}} \times \sum_{\substack{l,l'\\ m,m'}} f(r,r')_{Jll'}\, (ll'mm'|ll'Jm_J) \times Y_l^{m*}(\theta,\varphi)\, Y_{l'}^{m'*}(\theta',\varphi') \quad . \quad (2\text{-}13)$$

Next the exponentials are expanded using the expansion

$$e^{i\vec{k}\cdot\vec{r}} = 4\pi \sum_{l,m} i^l j_l(kr)\, Y_l^{m*}(\theta_k, \varphi_k)\, Y_l^m(\theta, \varphi) \tag{2-14}$$

where θ_k and φ_k are the spherical angular coordinates of $\vec{k}$. Then

$$\begin{aligned} m(\vec{k}, \vec{k}')_{Jm_J} = (4\pi)^2 \int d\vec{r} \int d\vec{r}' \sum_{l,m} i^l j_l(kr) \\ \times Y_l^{m*}(\theta_k, \varphi_k)\, Y_l^m(\theta, \varphi) \sum_{l',m'} i^{l'} j_{l'}(k'r') \\ \times Y_{l'}^{m'*}(\theta_{k'}', \varphi_{k'}') Y_{l'}^{m'}(\theta', \varphi') \sum_{ll'} f(r,r')_{Jll'} \\ \times \sum_{m,m'} (ll'mm' | ll'Jm_J)\, Y_l^{m*}(\theta, \varphi)\, Y_{l'}^{m'*}(\theta', \varphi') \end{aligned} \tag{2-15}$$

Integration over the space angular coordinates leads to

$$\begin{aligned} m(\vec{k}, \vec{k}')_{Jm_J} = (4\pi)^2 \int dr \int dr' \sum_{l,l'} f(r,r')_{Jll'}\, i^{l+l'} \\ \times j_l(kr)\, j_{l'}(k'r') \sum_{m,m'} (ll'mm' | ll'Jm_J) \\ \times Y_l^{m*}(\theta_k, \varphi_k)\, Y_{l'}^{m'*}(\theta_{k'}', \varphi_{k'}') \end{aligned} \tag{2-16}$$

where the orthonormal property of the spherical harmonics has been utilized. Equation (2-16) can be written in a more convenient form as

$$\begin{aligned} m(\vec{k}, \vec{k}')_{Jm_J} = \sum_{l,l'} a(k,k')_{Jll'} \sum_{m,m'} (ll'mm' | ll'Jm_J) \\ \times Y_l^{m*}(\theta_k, \varphi_k)\, Y_{l'}^{m'*}(\theta_{k'}', \varphi_{k'}') \end{aligned} \tag{2-17}$$

where

$$a(k,k')_{Jll'} = (4\pi)^2 i^{l+l'} \int dr \int dr' f(r,r')_{Jll'}\, j_l(kr)\, j_{l'}(k'r') \tag{2-18}$$

To evaluate $a(k, k')_{Jll'}$ it is necessary to make an assumption about the form of $f(r, r')_{Jll'}$. This function is defined in such a way that

it is zero for either $r > \lambda\!\!\!^{-}$ or $r' > \lambda\!\!\!^{-}$ where $\lambda\!\!\!^{-} = \hbar/m_\tau c$. This corresponds to the introduction of a momentum cutoff $k = 1/\lambda\!\!\!^{-}$ and $k' = 1/\lambda\!\!\!^{-}$. Thus the $a_{J\ell\ell'}(k, k')$ will have a contribution only for $r < \lambda\!\!\!^{-}$. In τ^+ decay

$$k \ll \frac{c}{\hbar}\sqrt{\frac{4}{3} m_\pi (m_\tau - 3m_\pi)}$$

always. This corresponds to

$$r k \ll \sqrt{\frac{4}{3}(m_\pi/m_\tau)\left(1 - 3\frac{m_\pi}{m_\tau}\right)} \approx 0.2$$

so it is possible to use only the leading term in the expansion for small kr

$$j_\ell(kr) \simeq (kr)^\ell/(2\ell+1)!!$$

To this approximation

$$a(k,k')_{J\ell\ell'} = (4\pi)^2 i^{\ell+\ell'} \int dr \int dr' f(r,r') \times \left[\frac{(kr)^\ell}{(2\ell+1)!!} \cdot \frac{(k'r')^{\ell'}}{(2\ell+1)!!}\right] \tag{2-19}$$

or

$$a(k,k')_{J\ell\ell'} = \alpha(r,r')_{J\ell\ell'} \cdot k^\ell k'^{\ell'} \tag{2-20}$$

where $\alpha(r, r')_{J\ell\ell'}$ is independent of k and k'. Then

$$m(\vec{k},\vec{k}')_{Jm_J} = \sum_{\ell,\ell';m,m'} \alpha(r,r')_{J\ell\ell'} \cdot k^\ell k'^{\ell'} (\ell\ell' mm' | \ell\ell' J m_J) \times Y_\ell^{m*}(\theta_k, \varphi_k)\, Y_{\ell'}^{m'*}(\theta'_{k'}, \varphi'_{k'}) \tag{2-21}$$

For a τ^+ decay in which the angle θ between $\vec{k}$ and $\vec{k}'$ and the magnitude of the momentum, k', are given then the kinematics of the final state are, of course, completely specified. The matrix element for decay into this state is then

$$|M(K',\cos\theta)|^2_J = \sum_{m_J} \int d\vec{k} \int d\vec{k}' |m(\vec{k}\,\vec{k}')_{J m_J}|^2 \qquad (2\text{-}22)$$

$$\times \delta(k'-K)\,\delta(k - k(k',\theta_{k'},\varphi_{k'},\theta_k,\varphi_k))\,\delta(\hat{u}\cdot\hat{u}' - \cos\theta)$$

where the m_J dependence is removed by summing over all m_J compatible with $m_J = m + m'$. Since the axis of quantization is arbitrary it can be taken to lie along a line with spherical angular coordinates $(\theta_{k'}, \varphi_{k'})$. Then (2-21) becomes

$$m(\vec{k}\,\vec{k}') = \sum_{l,l'} \alpha(r,r')_{Jll'}\, k^l k'^{l'} (ll'm_J 0 | ll'J m_J)\, Y^{m_J *}_l(\theta_k,\varphi_k)\, Y^0_{l'}(0,0)$$

$$= \sum_{l,l'} \alpha(r,r')_{Jll'}\, k^l k'^{l'} (ll'm_J 0 | ll'J m_J) \qquad (2\text{-}23)$$

$$\times \sqrt{\frac{(2l'+1)(2l+1)}{(4\pi)^2}}\; P_l^{m_J}(\cos\theta)\, e^{i m_J \varphi_k}.$$

So the integration over k gives

$$|M(K',\cos\theta)|^2_J = (4\pi) \sum_{m_J} \int \Big| \sum_{l,l'} \alpha(r,r')_{Jll'}\, k^l(k',\cos\theta)\, k'^{l'}$$

$$\times (ll'm_J 0 | ll'J m_J) \sqrt{\frac{(2l'+1)(2l+1)(l-|m_J|)!}{(4\pi)^2 (l+|m_J|)!}}$$

$$\times P_J^{m_J}(\cos\theta_k) \Big|^2 \delta(k'-K')\,\delta(\cos\theta_k - \cos\theta)\, d\vec{k}'$$

$$= (8\pi)^2 \sum_{l,l',m_J} \Big| \alpha(r,r')_{Jll'}\, k^l K'^{l'} (ll'm_J 0 | ll'J m_J) \qquad (2\text{-}24)$$

$$\times \sqrt{\frac{(2l'+1)(2l+1)(l-|m_J|)!}{(4\pi)^2 (l+|m_J|)!}}\; P_l^{m_J}(\cos\theta) \Big|^2 .$$

Replacing k and K' by p/ħ and p'/ħ respectively and dividing by the constants yields the distribution function

$$F_J(p';\cos\theta) = \sum_{m_J,\ell,\ell'} \Big| \alpha(r,r')_{J\ell\ell'}\, p^{\ell} p'^{\ell'} (\ell\ell' m_J 0 | \ell\ell' J m_J) \sqrt{\frac{(2\ell'+1)(2\ell+1)(\ell-|m_J|)!}{(\ell+|m_J|)!}}\, P_\ell^{m_J}(\cos\theta) \Big|^2 \qquad (2\text{-}25)$$

where $|\ell - \ell'| \leq J \leq \ell + \ell'$. The assumptions made in the derivation above are such that the lowest (ℓ,ℓ') pairs make the largest contribution to F_J. Thus, neglecting higher angular momentum terms

$$F_J(p';\cos\theta) = \sum_{m_J} \Big| \alpha(r,r')_{J\ell\ell'} \Big|^2 p^{2\ell} p'^{2\ell'} \Big| (\ell\ell' m_J 0 | \ell\ell' J m_J) \times \sqrt{\frac{(2\ell'+1)(2\ell+1)(\ell-|m_J|)!}{(\ell+|m_J|)!}}\, P_\ell^{m_J}(\cos\theta) \Big|^2 \qquad (2\text{-}26)$$

In obtaining equation (2-25) the only conservation law which has been used explicitly is the law of conservation of angular momentum. This restricts the values of ℓ and ℓ' which are allowed by requiring that they satisfy the triangle condition, $|\ell - \ell'| \leq J \leq \ell + \ell'$. The conservation of parity places a further condition on ℓ and ℓ'. This is that the states of ℓ and ℓ' which are summed over must be compatible with parity conservation in the sense described in Section 2.2. In Table III those values of (ℓ, ℓ') which are allowed by both the conservation of angular momentum and parity are listed. This table shows for each value of J and P of the τ meson the allowed (ℓ, ℓ') states which may occur in the final state. To the left of the dotted line are the pairs (ℓ, ℓ') corresponding to the minimum value of the quantum mechanical combinations of ℓ and ℓ' compatible with the choice of J and P. Examples of the higher order terms lie on the right. In Table IV the F_{JP}'s calculated by

taking only the first term, that is by using equation (2-26), are listed.

TABLE III

Allowed (ℓ, ℓ') Values for a τ Meson of Given J and P

J, P		Possible (ℓ, ℓ')
0 +1	----	----
0 -1	(0, 0)	(2, 2); (4, 4)...
1 +1	(0, 1)	(2, 1); (4, 3)...
1 -1	(2, 2)	(4, 4); (6, 6)...
2 +1	(2, 1)	(2, 3); (4, 3)...
2 -1	(0, 2); (2, 0)	(2, 4); (4, 2)...

TABLE IV

F_{JP}'s Calculated from Equation 2-26

J	P	F_{JP}
0	-	1
1	+	p'^2
1	-	$p^4 p'^4 \sin^2\theta \cos^2\theta$
2	+	$p^4 p'^2 \sin^2\theta$
2	-	$\lvert\alpha_{20}\rvert^2 p^4 + \lvert\alpha_{02}\rvert^2 p'^4 \pm 2\lvert\alpha_{02}\rvert\lvert\alpha_{20}\rvert p^2 p'^2(3\cos^2 -1)$

- - - -

It is convenient to write the F_{JP} in terms of new parameters $\epsilon = \frac{E_{\pi^-}}{E_{max}}$, where $E_{max} = 2/3\ Q$, and $x = 1\sqrt{3}\ (\epsilon_1 - \epsilon_2)$ where $\epsilon_i = E_{\pi_i}+/E_{max}$ and $\epsilon_1 > \epsilon_2$. From equation (2-5) it follows that $\cos\theta = \frac{x}{x_m} = \sqrt{\frac{1}{3}}\ \frac{\epsilon_1 - \epsilon_2}{\sqrt{\epsilon(1 - \epsilon)}}$.

For comparison with experimental data the functions $F_{JP}(\epsilon, x)$ must be normalized. That is

$$\frac{\int_0^1 \int_0^{x_m} F_{JP}(\epsilon, x)\, d\epsilon\, dx}{\int_0^1 \int_0^{x_m} d\epsilon\, dx} = 1$$

where $x_m = \sqrt{\epsilon(1 - \epsilon)}$. The normalized $F_{JP}(\epsilon, x)$ are given in Table V. Note that for the 2- case the values of A and B, which represent the weight of the contribution of the (2, 0) and (0, 2) states, are unknown.

TABLE V

Normalized Distribution Functions

J	P	$F_{JP}(\epsilon, x)$
0	-	$\pi/8$
1	+	$(\pi/4)\ \epsilon$
1	-	$24\pi\epsilon^2(1 - \epsilon)^2\ [1-(x/x_m)^2]\ \ (x/x_m)^2$
2	+	$2\pi\ \epsilon(1 - \epsilon)^2\ [1-(x\ x_m)^2]$
2	-	$(2/5)\ [\pi/(A^2+ B^2)]\ [A^2\epsilon^2 + B^2(1-\epsilon)^2 \pm 2AB\epsilon(1-\epsilon)(3\cos^2\theta-1)]$

- - - - -

where

$$\frac{\int_0^1 \int_0^{x_m} F_{JP}(\epsilon, x)\, d\epsilon\, dx}{\int_0^1 \int_0^{x_m} d\epsilon\, dx} = 1$$

The transition rate in terms of (ϵ, x) can now be written as

$$\frac{d^2R}{d\epsilon\, dx} = F_{JP}(\epsilon, x)\, \rho(\epsilon, x)$$

As a function of (ϵ, cos θ) it is

$$\frac{d^2R}{d\epsilon\, d(\cos\theta)} = F_{JP}(\epsilon, \cos\theta)\, \rho(\epsilon, \cos\theta).$$

The factor ρ is the volume in phase space, and it is in calculating this quantity that the conservation of energy and momentum are used explicitly. It is also assumed that the probability of a decay leading to a specified accessible volume of phase space is directly proportional to that volume. It can be shown that $\rho(\epsilon, x)$ is a constant and that $\rho(\epsilon, \cos\theta)$ is proportional to $\sqrt{\epsilon(1-\epsilon)}$. Thus the expression of the energy spectrum is

$$\frac{dR}{d\epsilon} = \int_0^{x_m} F_{JP}(\epsilon, x)\, dx$$

and that for the angular spectrum is

$$\frac{dR}{d(\cos\theta)} = \int_0^1 F_{JP}(\epsilon, \cos\theta)\sqrt{\epsilon(1-\epsilon)}\, d\epsilon$$

The results of these integrations are given in Table VI. Figure 3 and 4 are the resulting curves.

TABLE VI

Expressions for the Angular and Energy Spectra

J	P	$dR/d(\cos\theta)$
0	-1	1
1	+1	1
1	-1	$15/2\ \cos^2\theta\ \sin^2\theta$
2	+1	$3/2\ \sin^2\theta$
		$\frac{dR}{d\epsilon}$
0	-1	$8/\pi\ \sqrt{\epsilon(1-\epsilon)}$
1	+1	$16/\pi\ \epsilon\sqrt{\epsilon(1-\epsilon)}$
1	-1	$192 \times 16/15\pi\ \epsilon^2(1-\epsilon)^2\sqrt{\epsilon(1-\epsilon)}$
2	+1	$(16)^2/3\pi\ \epsilon(1-\epsilon)^2\ \sqrt{\epsilon(1-\epsilon)}$

- - - - - -

2.4 The τ^+ Decay Spectrum When Parity is not Conserved in the Decay

When the conservation of parity is not assumed in the τ^+ decay, equation (2-25) is still valid and the only restriction placed on the (ℓ, ℓ') pairs is that which arises from the conservation of angular momentum. The distribution function will now be a sum of contributions from (ℓ, ℓ') substates of both parities. The amount with which each of the two parity states contributes to the distribution function obviously depends on the form of the decay interaction. However, if the Dalitz-Fabri model is to be preserved, it must still be assumed that the lower (ℓ, ℓ') terms constitute the major contribution to the spectrum. Since nothing is known about the form of the parity non-conserving decay interaction the spectrum will only be discussed

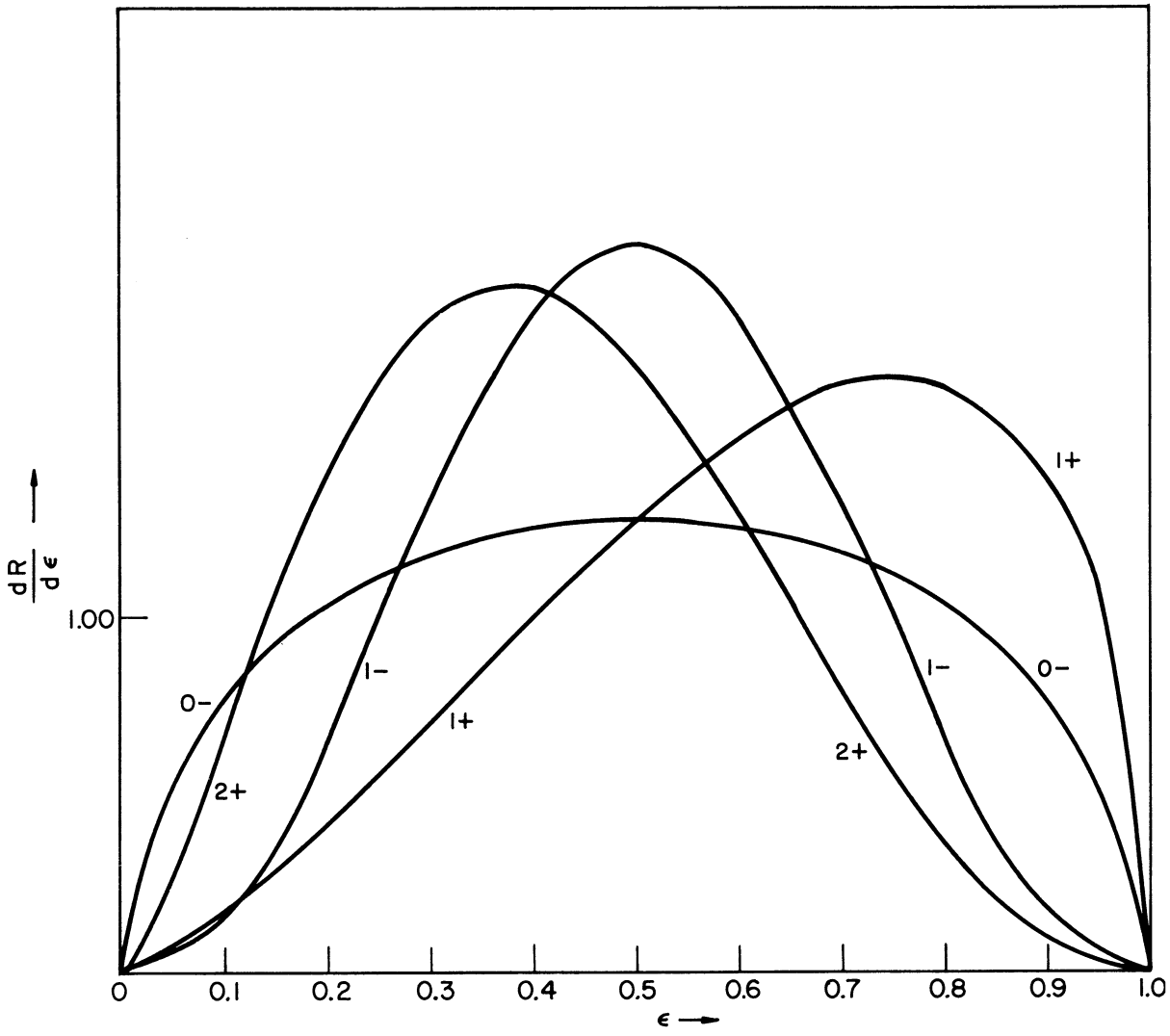

FIG. 3.
Energy spectra for spin-parity combinations ($S \leq 2$) as predicted by Dalitz - Fabri theory.
2- is not shown.

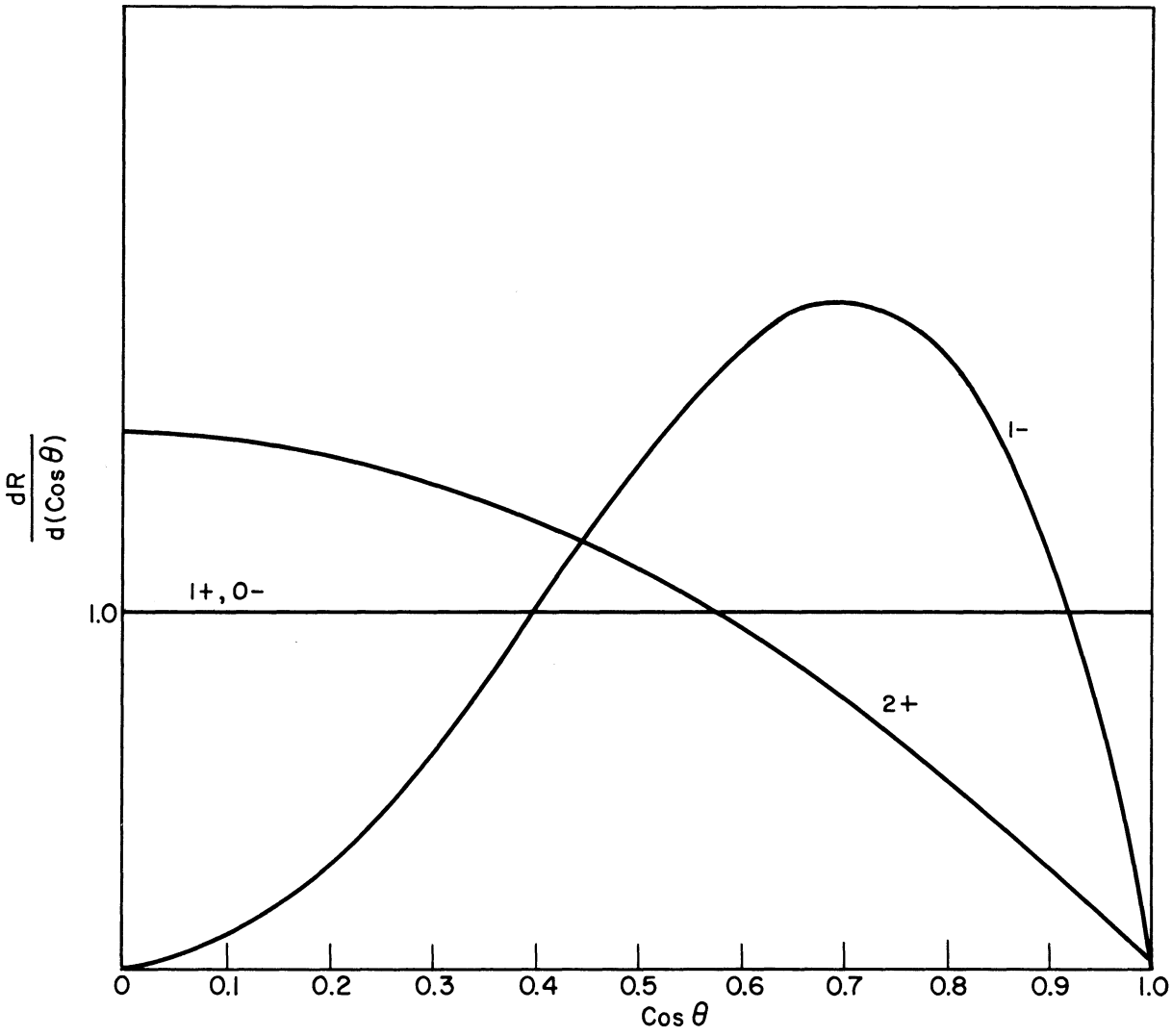

FIG. 4.
Angular spectra for spin-parity combinations ($S \leq 2$)
as predicted by Dalitz – Fabri theory.
2- is not shown.

on the basis of the following two assumptions:

(1) The form of the interaction is such that no final substate is favored by virtue of its parity, that is, the interaction is parity independent.

(2) The magnitude of the contribution from the various (ℓ, ℓ') terms in a given distribution function decreases as (ℓ, ℓ') increases.

The requirement that ℓ be even is not relaxed, of course.

The spin zero distribution function will be the same as that given previously for (0-) since only one parity state can be formed for this value of the spin. The major contribution to this distribution function arises from the term in which the (ℓ, ℓ') pair is (0, 0). Reference to Table III shows that the next term corresponds to (2, 2) and is assumed to be very small. For spin one, the spectrum will be the same as that previously given for (1+) since the lowest term is (0, 1) and the next lowest term (2, 1) is from the same parity state. It is not until the third term that an (ℓ, ℓ') pair corresponding to an opposite parity state can contribute. For spin two the (2, 1) pair might be included with the (0, 2) and the (2, 0) pair to given a spectrum different from the 2+ or 2- spectrum. This leads to a function of the form

$$F(p', \cos\theta) = |\alpha_{20}|^2 p^4 + |\alpha_{02}|^2 p'^4 \pm 2|\alpha_{02}||\alpha_{20}| p^2 p'^2 (3\cos^2\theta - 1) + \frac{2}{3}\left(\frac{32}{35}\right)^2 |\alpha_{21}|^2 p^4 p'^4 (1 - \cos^2\theta)$$

where the α's are unknown and must be adjusted to fit the experimental distribution. Lomon[22] has considered this spectrum and the spectrum

from other spins with parity non-conservation. The agreement of the spectrums with the experimental data is not improved for odd spins or for spin zero. For spin two better agreement can be attained but this is because there are so many arbitrary constants to adjust. However, unless the precision and statistics of the spectrum measurements are considerably improved it is doubtful that it can be shown to be necessary to introduce parity non-conservation in the τ^+ decay on the basis of the τ^+ spectrum itself without considering the θ^+ decay mode.

CHAPTER III

EXPERIMENTAL APPARATUS AND PROCEDURE

3.1 The K^+ Meson Beam

The K^+ mesons for this experiment were obtained by bombarding a 3 inch thick copper target with the 3 Bev external proton beam of the Cosmotron at the Brookhaven National Laboratory. If only K^+ mesons were produced in this bombardment an experimentally useful beam of such particles could be formed rather easily. A magnetic system incorporating vertical and horizontal focussing in addition to momentum separation could be placed so as to accept a certain solid angle of the charged reaction products and those products of correct momentum could then be focussed at the detector chosen for the experiment. In fact, among the charged reaction products the π^+ mesons are more plentiful than the K's by a factor of about one hundred. Thus, since the π^+ meson has a lifetime comparable to that of the K^+, a beam formed by such a magnetic lens system would be mostly π^+ mesons. Since the method of detection chosen for this experiment is essentially a visual one it is necessary to keep the number of particles which arrive at the detector per Cosmotron pulse below a maximum of about 20. This can be achieved by an ordinary analysis-focussing system by decreasing the number of protons in the initial external beam. Such a resolution of this difficulty has the disadvantage that it results in only one K^+ meson in about 40 Cosmotron pulses, i.e., about 3.33 minutes. It should be pointed out that although protons are among the collision products the range of those reaching the detector via the analysis system is such that they are

stopped in the wall of the detector and therefore do not constitute a background problem.

The problem introduced above was solved by using a two magnet system with an absorber between the magnets. This system was designed by Dr. Donald I. Meyer and is illustrated in Figure 5. In this system the momentum analyzed beam of π^+ and K^+ mesons is brought to a focus at a 3 inch Be moderator. In traversing this moderator the K^+'s lose more momentum than do the π^+'s. The second analyzing magnet is placed after the moderator, and the detector is placed at the focal point of this second magnet which corresponds to the post moderator momentum. In such a system it is necessary to keep the distances as short as possible so that the number of K^+ mesons lost from the beam is kept at a minimum. This was accomplished by combining strong focussing with momentum analysis in the same magnet.[23] By using a large gradient both horizontal and vertical focussing were obtained with a 3 meter object to image distance for each magnet. In Figure 6 a plot of the beam obtained from this system is drawn. The historgrams were obtained by plotting the end points of the stopping τ meson tracks, excluding those which suffered large angle scatterings. In all three histograms 90% of the beam lies between the dashed lines. Using this system it was possible to obtain one K^+ meson in about 6 Cosmotron pulses, i.e., about 30 seconds and, in all, about 3500 K^+ mesons were observed in the course of the experiment.

3.2 The Detecting Device

A propane (C_3H_8) bubble chamber with sensitive volume 12 x 12 x 30 cm was the detecting device utilized in this experiment. The operating

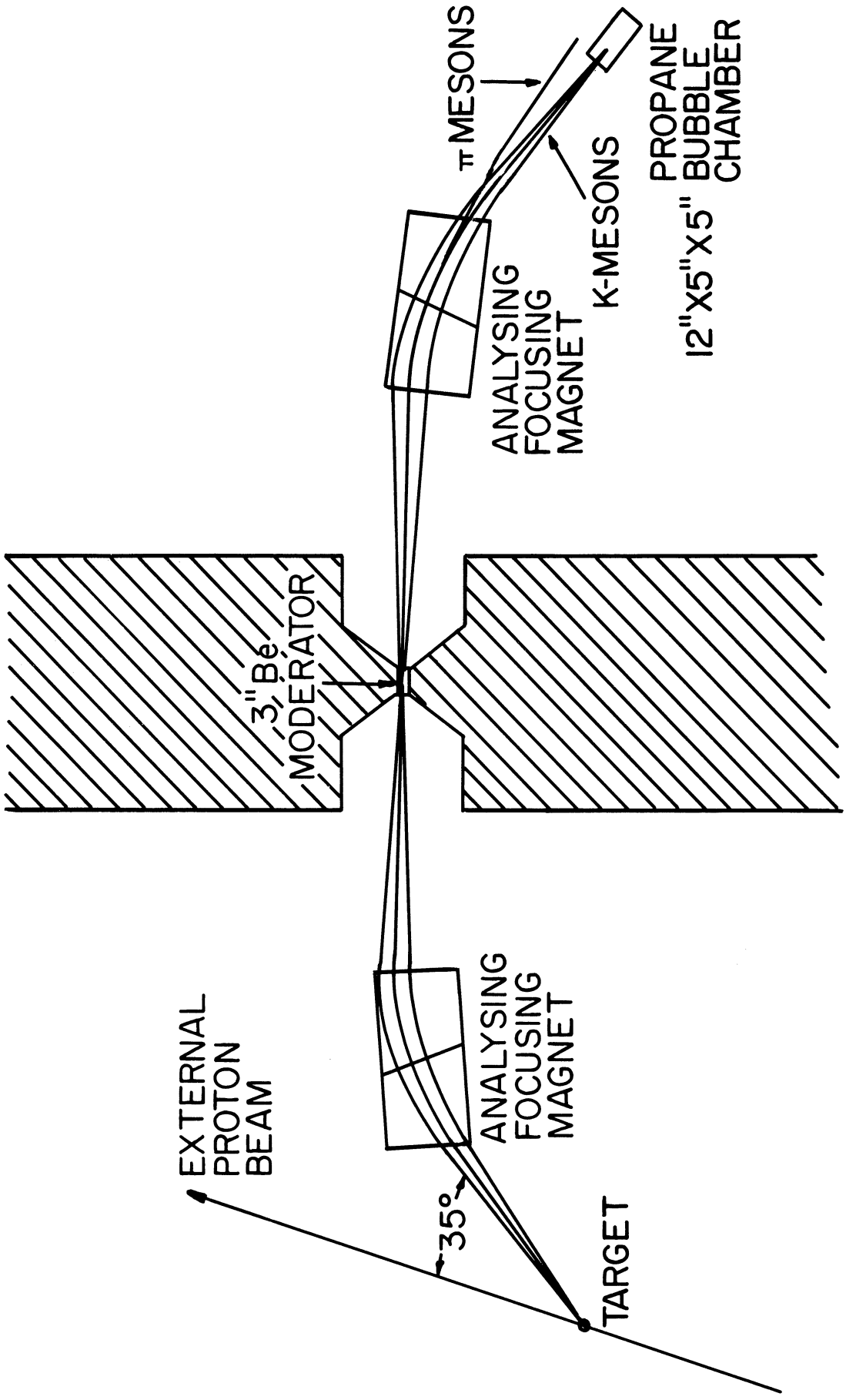

FIGURE 5. PLAN VIEW OF EXPERIMENTAL SETUP

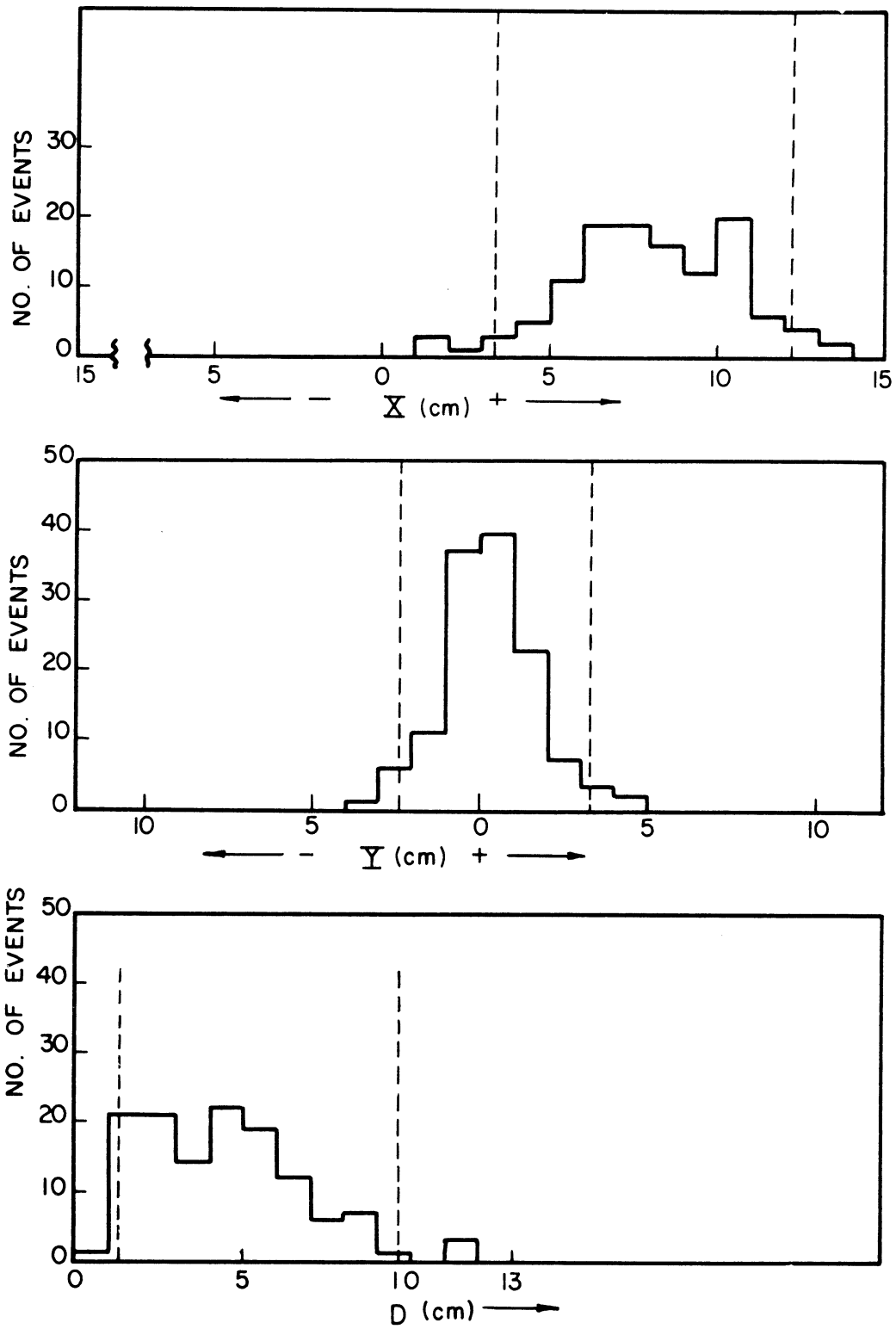

FIGURE 6 Plot Of Beam X Y D Distributions

temperature of the chamber was 52.8°C. Figure 7 shows end and top views of the chamber. The main body of the chamber is of aluminum and the compressed propane is expanded by means of a diaphragm located in a throat at the bottom of the chamber. Full details of bubble chamber construction and operation are discussed adequately elsewhere and will not be considered here.[24]

The events occurring in the chamber are photographically recorded on 70 mm film by two cameras set at approximately a 15° stereo angle. The film was held flat by means of pressure plates and vacuum backs in these cameras. Two Xenon filled flash tubes act as a light source for bright field photography. The duration of the flash was approximately 40 μs. The iris diaphragms of the cameras were set at f45 and this provided depth of field sufficient to yield fairly good focus in all parts of the chamber. The camera was supported rigidly by an I beam structure after focussing and levelling. The arrangement of the cameras and the illumination system is illustrated in Figure 7.

In order that events may be reconstructed from the stereo views it is necessary to establish a coordinate system in the chamber. This was accomplished by a regular rectangular grid of fiducial marks printed on the front and back windows. These were carefully aligned by means of a surveyor's transit prior to the experiment.

In Figure 8 the two stereo views of an event are shown. The top picture is the view of the chamber as seen by the upper camera, and the bottom is that of the bottom camera.

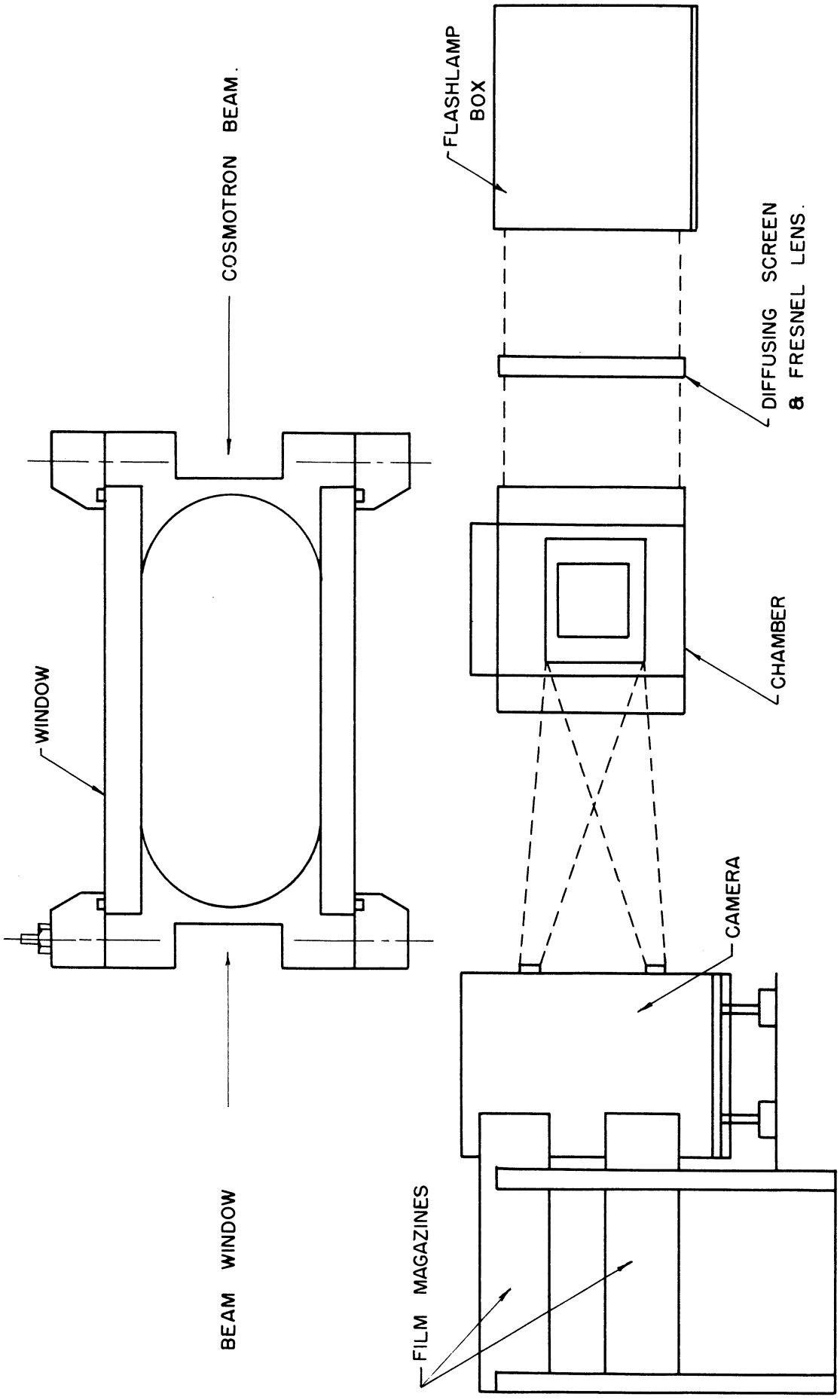

FIGURE 7. END AND TOP VIEWS OF BUBBLE CHAMBER

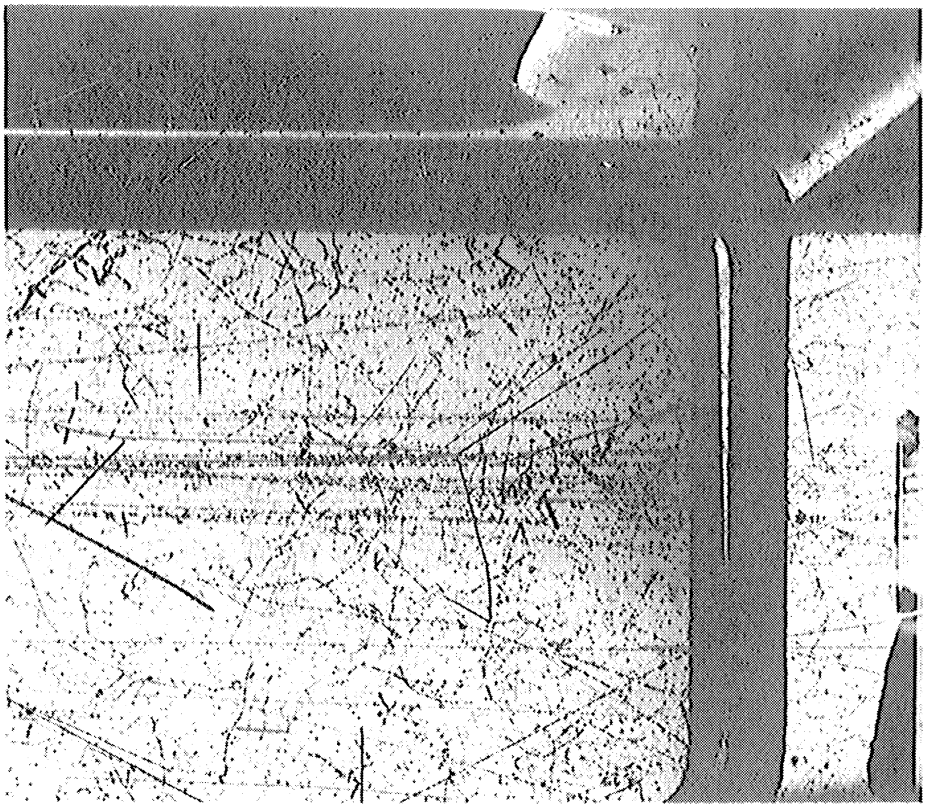

Top View

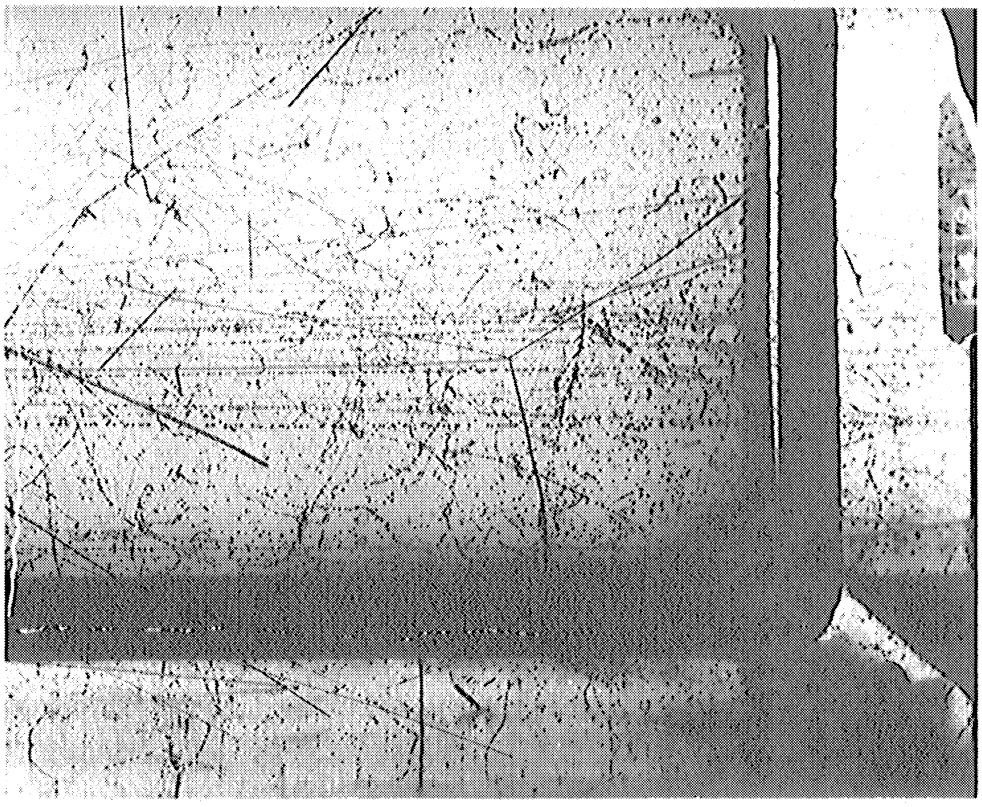

Bottom View

Figure 8. Stero Views of an Event

3.3 The Scanning Procedure

About 25,000 pictures were taken and of these 20,400 were scanned. The remainder of the pictures were not scanned because of excess beam intensity, no beam being present, or damage to the film in the developing process. The large size of the film made it possible to scan the pictures with the aid of only a hand magnifier of 6.5x magnification. Since the tracks in the chamber are produced by particles of the same momentum and since the only beam particles reaching the chamber are μ, π or K mesons it follows that the heaviest particles, that is, the K's, will produce the tracks with the highest bubble density.[25] The scanning was done by looking first along the entrance of the chamber. Those tracks having higher bubble density were then followed into the chamber. Decay into a lightly ionizing secondary or into the characteristic τ^+ mode served to identify the K^+ meson. Since K^+-proton[26] and K^+-nucleus[27] scattering cross-sections were to be obtained from these pictures great care was taken to identify all of the K^+ particles. However, except for the τ^+ decay mode no attempt was made to identify the various types of K^+ mesons. It should be emphasized that in the scanning both stereo views were used. This gives the scanner the ability to observe an event from two viewing points. This tends to increase the scanners' efficiency for certain types of events. In particular, τ^+ decays in which the π^- meson has a very short track are often detected only after a look at both stereo views.

A check on the reliability of the scanning was made by carefully rescanning about 3,000 of the pictures. In this rescan only one

new τ event was found. This event was unusual in that it scattered through a large angle immediately after entering the chamber, and the decay occurred near the bottom of the chamber. The important result of the rescanning appears to be that it is unlikely that τ's were missed if they came to rest in the chamber without suffering a large angle scattering while traversing the first few centimeters of the chamber. It is estimated that better than 90% of the τ mesons present have been found in the scanning.

In all, 189 possible τ mesons were found in the scanning of the pictures. For a portion of the run the top camera did not function properly and stereo views were not obtained for all of the pictures. At the end of the run the beam intensity increased intermittently making accurate identification and measurement difficult in a large number of cases. To avoid sample bias and error, therefore, all of these events were discarded. This corresponded to approximately 3000 pictures, or about 28 τ events. Thus there remained 161 possible τ mesons which could be subjected to measurement and analysis.

3.4 Reconstruction of Events

In Figure 9 the geometry of the stereo camera-bubble chamber system is illustrated. The two film surfaces are plane and parallel and the distance between optic axes of the two camera lenses is 2W. The coordinate system on film 1 is (x, y) and that on film 2 is (x', y'). S and S' are the distances between the lenses, 1 and 2, and the front window of the bubble chamber, which has thickness d, while v and v' are the distances between the lenses and their respective film planes. The

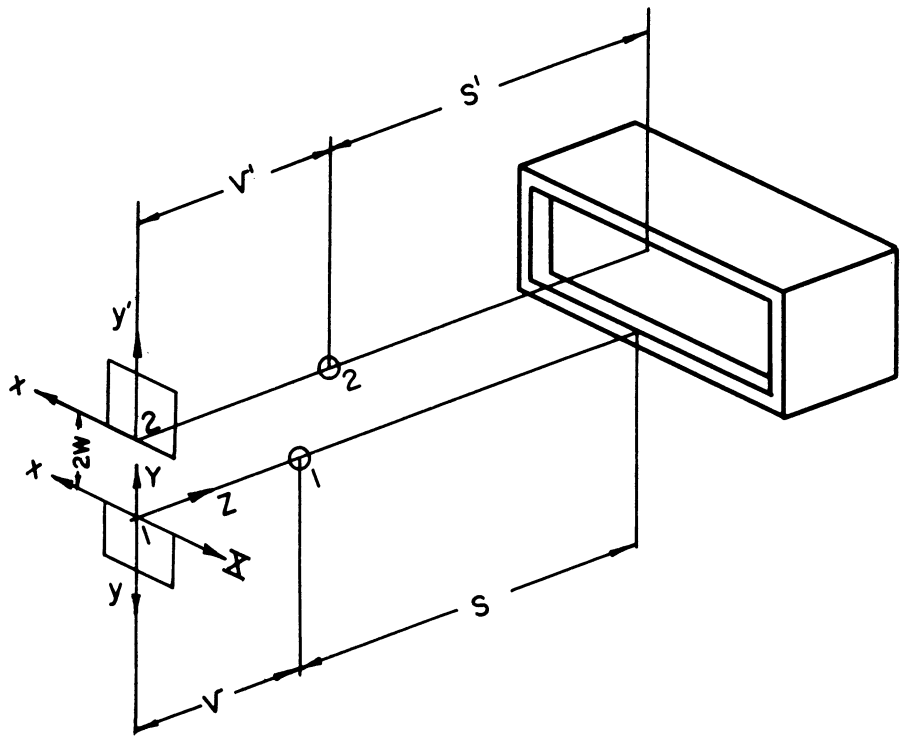

FIGURE 9 Stereo Camera – Bubble Chamber System

coordinates of a point P in the bubble chamber are taken to be X, Y, and D, where D is the perpendicular distance from the inside plane of the front window to P. The origin of the coordinate system is taken to lie on the optic axis of lens 1. X, Y, and D can be written in terms of the film coordinates as[28]

$$X = (x/v)(S + dT + UD) = (x'/v')(S' + dT' + DU')$$

$$Y = (y/v)(S + dT + UD) = 2W - (y'/v')(S' + dT' + DU')$$

$$D = \frac{2W - (y/v)(S + dT) - (y'/v')(S' + dT'')}{(y/v)U + (y'/v')\,U'} \qquad (3\text{-}1)$$

where

$$T = \left[n_1^2(\alpha^2 + 1) - \alpha^2\right]^{-1/2}$$

$$T' = \left[n_1^2(\alpha'^2 + 1) - \alpha'^2\right]^{-1/2}$$

$$U = \left[n_2^2(\alpha^2 + 1) - \alpha^2\right]^{-1/2}$$

$$U' = \left[n_2^2(\alpha'^2 + 1) - \alpha'^2\right]^{-1/2}$$

in which n_1 and n_2 are the indices of refraction of glass and propane respectively and where

$$\alpha^2 = \frac{x^2 + y^2}{v^2} \quad ; \quad \alpha'^2 = \frac{x'^2 + y'^2}{v'^2}$$

The quantity α (or α') entering here is actually the tangent of the angle between the optic axis and a ray passing through the center of the lens and then intersecting the film plane at the point (x, y) or (x', y'). For the chamber used in the present experiment α and α' have maximum values of about 1/3.

These equations can be put in a more useful form by rewriting them as

$$\begin{aligned} X &= x(P + DQ) = x'(P' + DQ') \\ Y &= y(P + DQ) = 2W - y'(P' + DQ') \end{aligned} \qquad (3\text{-}2)$$

where

$$P = \frac{S + dT}{v}, \quad Q = \frac{u}{v}$$

$$P' = \frac{S' + dT'}{v'}, \quad Q' = \frac{u'}{v'}.$$

Expanding T, T', U and U' gives, to first order in α or α', the constants

$$T = T' = 1/n_1$$

$$U = U' = 1/n_2.$$

Making use of the accurately known distances between the inside surfaces of the front and back windows and between the grid marks on each of these surfaces it is now possible to determine the values of P, P', Q, and Q'. This evaluation was carried out by C. Graves.[28] It is important to note in equations (3-1) and (3-2) that while the y coordinates on both films, that is, y and y', need to be measured, it is necessary to measure the x coordinate on only one of the films to determine the coordinates (X, Y, D). Furthermore, it should be borne in mind that these equations represent the special case in which the optic axis of lens 1 passes through the origin of coordinates. If another origin is to be chosen in the measuring process then a correction must be applied.

The measurement of the events is accomplished by means of a twin objective traveling microscope. In this instrument the film is clamped securely in place on a movable stage. The stage and the objective each

have one degree of freedom, and their directions of travel are at right angles. Thus by moving both the stage and the objective it is possible to view any point on the film. The eyepieces of the microscopes have cross hairs and the measurement of a point is accomplished by setting these cross hairs on the bubble of interest. The position of the cross hairs can then be read from a scale graduated to 1/1000 of an inch.

A schematic diagram of τ^+ meson decay is given in Figure 10. In this hypothetical decay the three types of tracks which occur most frequently have been drawn. These are the π^- track with a one prong star at its ending, the curved track arising from multiple coulomb scattering and the single large angle scattering. In the case of a straight track only two points on the track are measured. When a star occurs the length of its prongs are always measured. In the situation where a large angle scattering occurs the vertex point and the end point of the track were measured. If the pre-scattering portion of the track did not appear to be straight an intermediate point was also measured. The badly curved tracks represented the most difficult measuring problem. In this case the angles which are calculated may not be reliable so it is extremely important that an accurate length measurement be available. The method used was to measure points along the track sufficiently close together so that the angle between the chord connecting two adjacent points and the tangent to the track at the first point is extremely small. On some tracks it was necessary to measure as many as six points along the track. When $\pi^+ \rightarrow \mu^+ \rightarrow e^+$

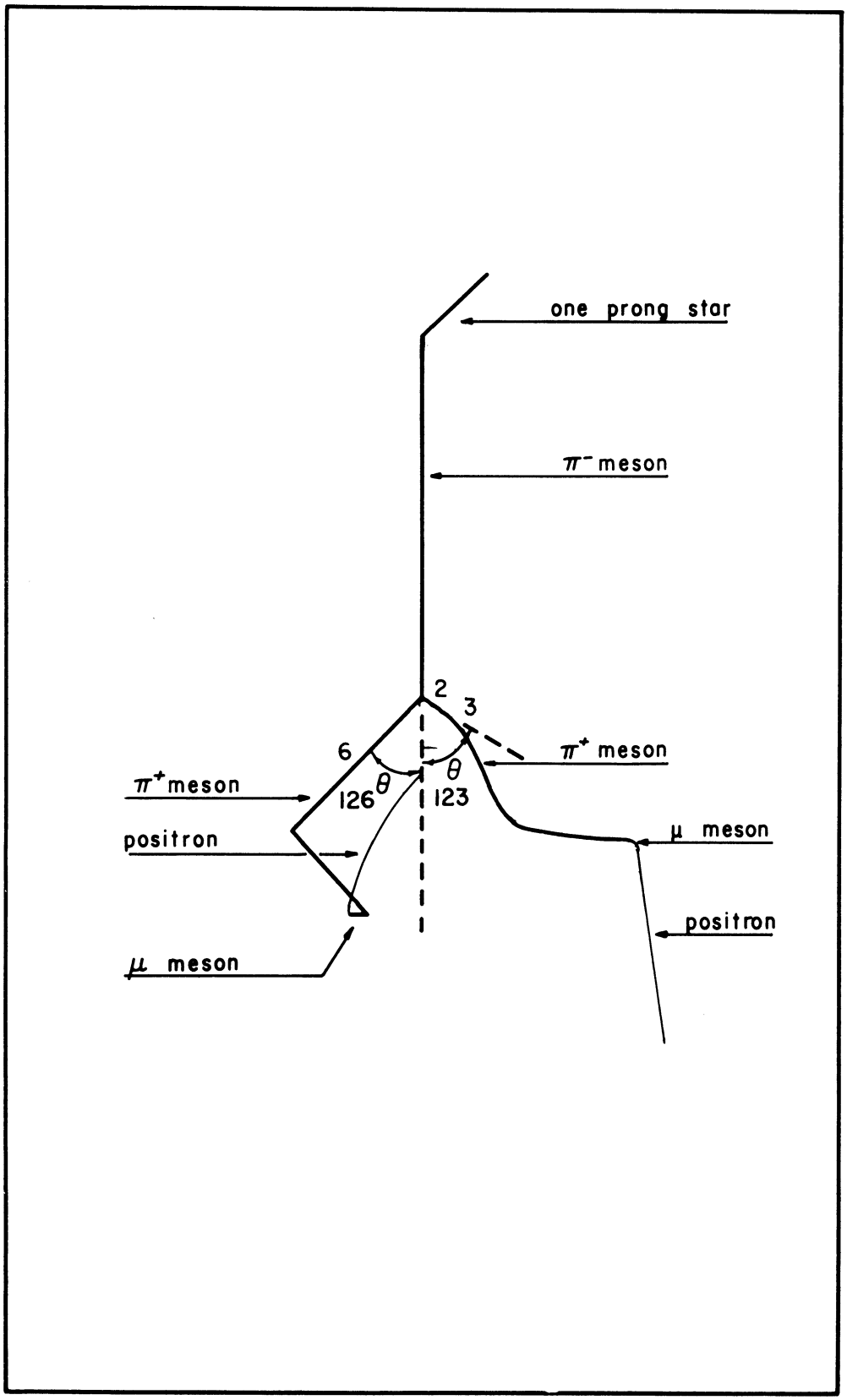

FIGURE 10 Diagram of τ Meson Decay

decays occurred in the chamber the coordinates of the beginning and of the end of the μ^+ track were also measured.

To reduce the chance of a measurement error occurring the events were measured two times before any reconstruction was attempted. These measurements were made at times fairly close together and thus the possibility of two repeated errors through "memory" of the event is not ruled out. As a check for such an effect about one-half of the events were remeasured a third time at a later date. No discernable effect was observed. If the results of the first two measurements did not agree with each other then two more measurements were made. In all cases it was possible, by careful checking, to resolve the difference.

The coordinates obtained by the measurements are then punched on IBM cards. To check against error in this process the cards were run through an IBM Card Verifier. The IBM 650 computer was programmed to calculate the coordinates of the points by means of equations (3-2). In addition to calculating the coordinates the machine was also programmed to compute the lengths of all tracks, the angles θ_{123} and θ_{126} shown in Figure 10, and the degree of coplanarity of the three pion tracks.

3.5 Analysis of the Events

It was pointed out in Chapter II that in a 3 body decay from rest, such as τ^+ meson decay, the momentum vectors of the decay products must be coplanar. The use of this fact and the knowledge of the Q value reduces the requirements of momentum and energy conservation to three equations in five variables. These can be the individual

momenta of the three π mesons and the angles θ_{123} and θ_{126} shown in Figure 10. Thus the knowledge of any two of these variables can completely determine the kinematics of the event.

For use in the analysis the values of p_1, p_2, and p_3 were computed by choosing the values of θ_{123} and θ_{126}. In this computation θ_{123} was held fixed and θ_{126} was varied in 3° increments, to include all possible decay configurations for the value of θ_{123}, then θ_{123} was increased by 3° and θ_{126} varied again. This process was repeated until all possible configuration had been considered. The Q value assumed in these calculations was 75 Mev. The results were then plotted and the resulting curves provided the kinematical information used in analyzing the data.

In the analysis of a particular event the first requirement used was that of coplanarity. The angle of coplanarity is obtained by taking the arcsin of the inner product of a line in the decay plane and the normal to the decay plane. In the several measurements that were made of an event the average value of this angle was required to be less than 5° for the event to be considered a decay from rest. When all three decay products were such that they stopped in the chamber the average measured value of the length of these tracks was sufficient to specify the event by means of the range energy relations. However, the further requirement was added that these values of the energy must be consistent with those obtained from measured average values of the angles using the kinematics curves. When one of the π mesons produced in the decay escapes from the chamber the range of the two remaining pions is sufficient to determine the kinematics of the

event, but again, the energy values so obtained were required to be consistent with those obtained using the angular measurements. In the third case, that is, when two of the pions escape leaving the third to come to rest in the chamber, the analysis must be done solely by means of the kinematics curves with the measured range of the pion acting only as a consistency check. In this experiment the majority of the events fall into the second category, that is, when two pions come to rest in the chamber.

When the π^- meson comes to rest in the propane it interacts predominantly with the carbon nucleus.[29] The reaction which takes place is

$$\pi^- + C^{12} \rightarrow 2\alpha + 1p + 3n$$

The experimental work of Ammiraju and Lederman[30] has shown that the majority of the α particles have energy less than 5 Mev. An α particle of this energy does not produce a track of sufficient length to be observable in a propane bubble chamber. The protons, however, are observed to have high energy tracks somewhat more frequently, and these can be observed. The secondary particles resulting from π^- interactions with propane were in all cases consistent with the results of Ammiraju and Lederman for hydrocarbons. It should be emphasized that the knowledge of the angles θ_{123} and θ_{126} serves to distinguish, in most cases, the single prong star from a pion scattering since the kinematics give the range of the pion. Thus, if the prong begins at the limit of the pion range then the prong is definitely an interaction product. On the other hand, if the pion track length

plus the prong length are greater than the pion range then the event is most probably an interaction in flight. In all cases which were observed in this experiment only one ambiguous situation arose and in this case the π^- probably interacted in flight. A further point to be mentioned is that although it is not always possible to distinguish a meson from a nucleon by bubble density and scattering it is almost always possible to distinguish an electron by means of these techniques.

3.6 Experimental Errors

In most treatments of experimental errors the various errors which may occur in the process of collecting and analyzing the data are grouped into two categories. The first type are referred to as the systematic errors while the second are the random errors. The systematic error is defined as an influence of approximately constant magnitude on the experimental data which is inherent in the process of obtaining the data. In an experiment such as this one systematic errors might be introduced if, for example, there was an error in the graduated scale of the measuring instrument or perhaps if the range energy curves were improperly computed. Random errors are those errors introduced into the data by a large number of irregular and fluctuating causes. Examples of these might be the thermal expansion or contraction of the film due to temperature variations during the measurement, or vibrations of the measuring instrument due to mechanical noise in the building.

In point of fact, most experimental errors are neither purely systematic nor purely random, but rather constitute a mixture of the two types. As an illustration of this point consider the fundamental

type of measurement involved in an experiment of this sort, that is, the measurement of the coordinates of a bubble. For purposes of illustration the geometric center of the image of the bubble on the film will be assumed to be the ideal point to measure. Now, if the measureer consistently chooses some point other than the center there will be a systematic error which will be equal to the distance from the "correct" point to the measured point. The random error arises from the fact that in a large number of measurements the experimenter is not able to set the cross hairs of the microscope exactly on the point of the bubble that he desires to measure but rather will obtain a distribution of measured coordinates about the ideal point.

The random error will fluctuate from observation to observation and hence cannot be precisely evaluated. Thus errors of this type may be regarded as random variables and treated by the methods of probability theory. Systematic errors, on the other hand, are approximately constant in their influence on the data and thus must either be eliminated or precisely evaluated.

In an experiment of this sort a check for systematic errors can be made by measuring a known constant which is not connected with the analysis to be carried out in the experiment. The data in this experiment contains two such independent checks. One comes from the reaction $\pi^+ \rightarrow \mu^+ + \nu$, where the π^+ is at rest and the μ^+ has a constant range corresponding to 4.17 Mev kinetic energy. Measurements were made on these μ^+'s which appeared in almost all orientations and positions in the chamber. Each μ^+ track was measured at least twice and the average value of these measurements was plotted. In all,

132 μ^+ tracks were measured. The results of these measurements is plotted in Figure 11. The value of the μ^+ length obtained by taking the mean from this plot is

$$\ell_\mu(\text{cm}) = 0.29 \pm 0.03 \text{ cm}.$$

If the density of propane is assumed to be 0.45 gm/cm^3 then

$$\ell_\mu(\text{gm/cm}^2) = 0.13 \pm 0.1 \text{ gm/cm}^2.$$

From the range-energy curves this is seen to correspond to

$$E_\mu = 4.2 + 0.2 \text{ Mev}$$

which is consistent with the known value of the μ^+ kinetic energy.

The second check is found in the elastic scattering $K^+ + p \rightarrow K^+ + p$. These events should also be coplanar since the proton is initially at rest in the propane. The data on these events were measured by Drs. M. L. Perl and D. I. Meyer, Thirty-two elastic scatterings were observed and, of these 23 of them had measured coplanarity angles of less than 5°. These data are plotted in Figure 12. It seems to be possible to explain the existence of the remaining nine events with coplanarity angle greater than 5° as being due to poor photography, extremely short recoil tracks, or an orientation of the scattering plane which makes measurement exceedingly difficult.

The existence of strong internal consistency in this experiment provides somewhat weaker evidence for the absence of systematic error. In particular, no event was found in which the results obtained by the use of the kinematics curves and the angular measurements were different from those obtained by using the range-energy curves and the length measurements.

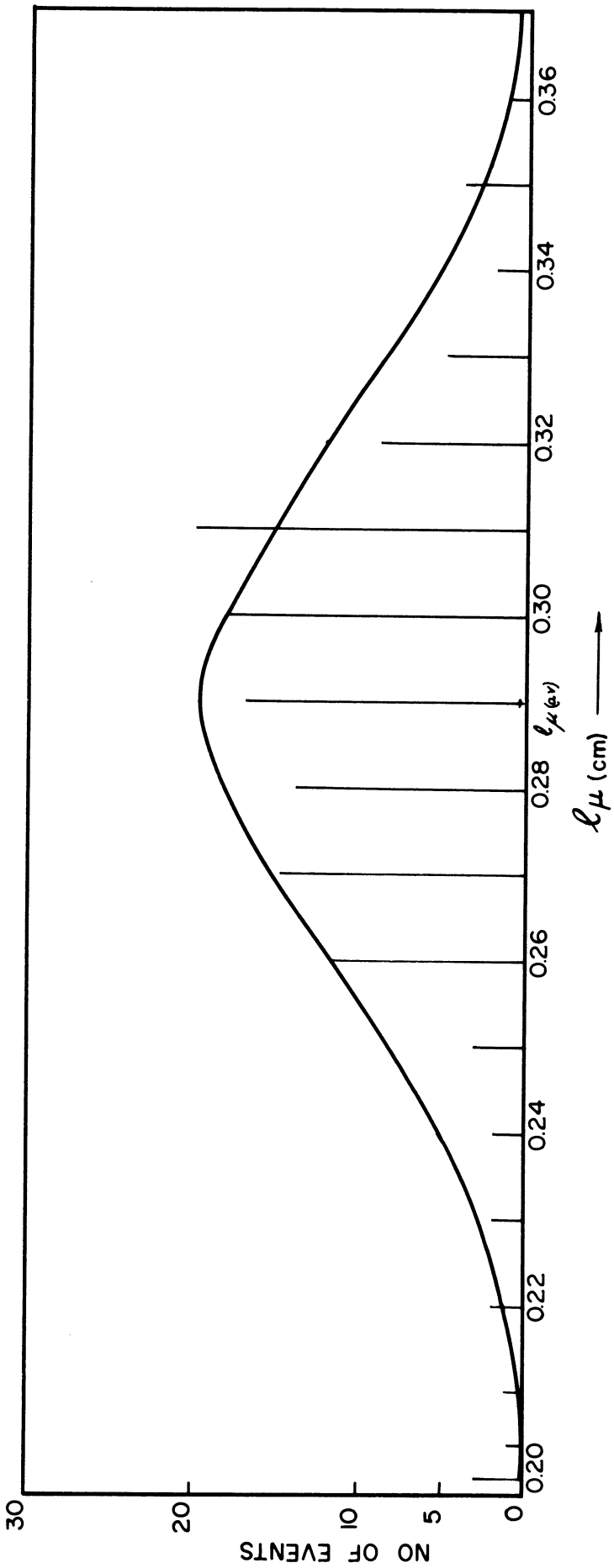

FIGURE II Measured μ^+ Lengths And Corresponding Gaussian

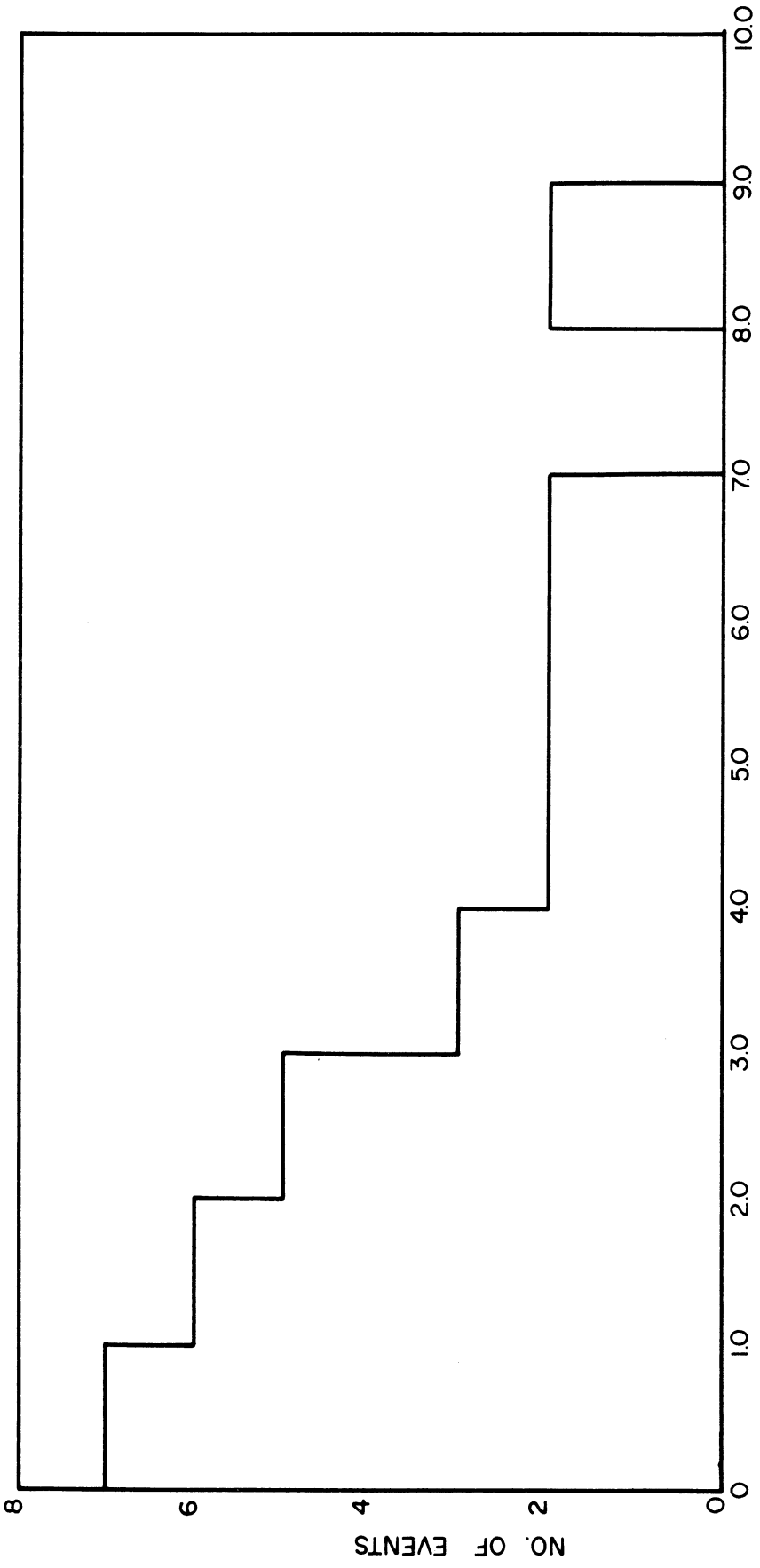

FIGURE 12 Plot Of K^+-p Scattering Coplanarity Angles

From the amount of consistency among the energy values from several measurements and between the values obtained by two different methods of analysis it is estimated that the error in the energies of the pions is approximately $\pm$ 1 Mev.

CHAPTER IV

DISCUSSION OF EXPERIMENTAL RESULTS AND CONCLUSIONS

4.1 Description of the Data

In Section 3.3 it was stated that 161 possible τ^+ decay events were found in the scanning. Fine scanning and preliminary analysis showed that six of these events were not τ^+ mesons. There were six cases of possible τ^+ mesons scattered throughout the data in which either the film was badly damaged or the photography was extremely poor. In these cases reliable measurement and analysis was not possible so the events were discarded. Since these events represent isolated instances at intervals of always at least 3,000 good pictures it is very improbable that the discarding of these events introduces any appreciable bias. Measurement showed that 13 of the events were decays in flight, and these also were not analyzed. Thus there remained 136 τ^+ meson decays from rest which could be analyzed.

The analysis of the decays from rest produced 111 cases of τ^+ mesons in which the energy of the 3π-mesons was determined by both the range-energy and the angular-kinematics method. The remaining 25 cases represent situations in which the identity of the π^- is uncertain. In these cases one of the π^+ mesons comes to rest and undergoes decay in the chamber while the other two particles escape through the walls. The knowledge of the angles gives the energies of the three pions, and this assignment is confirmed by the knowledge of the range of one of the π^+ mesons. In seven of these twenty-five cases the energies of the two unidentified pions are within three Mev of each other. The average of

these energies was taken to be the π^- energy. This leaves 118 cases in which the π^- energy and the cos θ are determined. The energy spectrum of these 118 cases is plotted in Figure 13, and the angular spectrum appears in Figure 14. Note that since cos θ is a derived quantity determined from ϵ, ϵ_1 and ϵ_2 it has an error associated with it which is equal to the combined errors in these quantities. This error in cos θ is approximately 0.06.

The 18 cases in which the π^- is not identified will be treated in the next section. In the appendix the complete data on all 136 cases is given in tabular form.

4.2 Comparison of the Data with the Theoretical Distribution Functions

In Chapter II the distribution functions for τ^+ decay were introduced. In this section these distribution functions will be compared with the experimental data. These comparisons will be made by means of certain statistical procedures which will now be introduced.

The first type of statistical test which will be applied to the data will be a relative probability test. This test employs the fact that the distribution function $F_J(\epsilon, x)$ is simply a probability density, that is, the probability of a set of N random events is proportional to $\prod_{i=1}^{N} F_J(\epsilon_i, x_i)$. If, however, there is no a priori reason to prefer one of the two distribution functions it may be possible to conclude that the observed data is more probable on the basis of one distribution function than on the basis of the other by considering the relative probability of the one to the other. For example, if $F_J(\epsilon, x)$ and $F_{J'}(\epsilon, x)$ are the distribution functions in question then

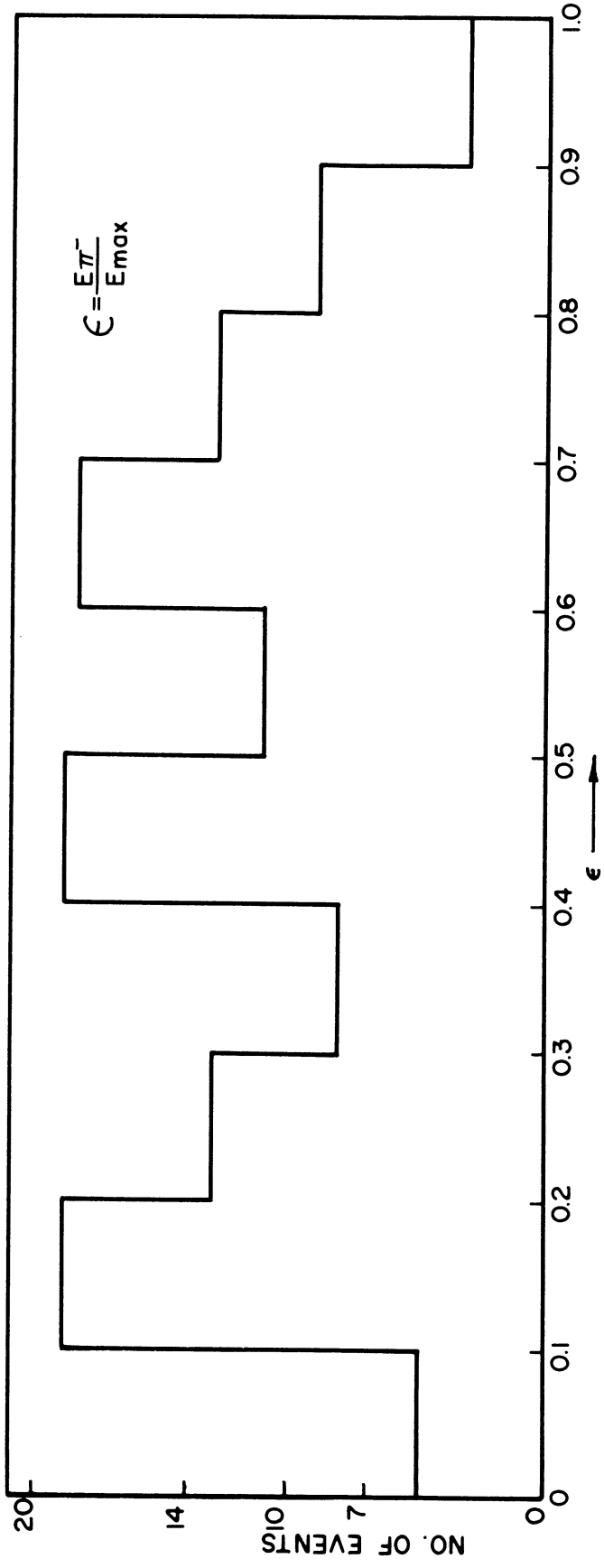

FIGURE 13 Experimental Energy Distribution For 118 Unambiguous Events

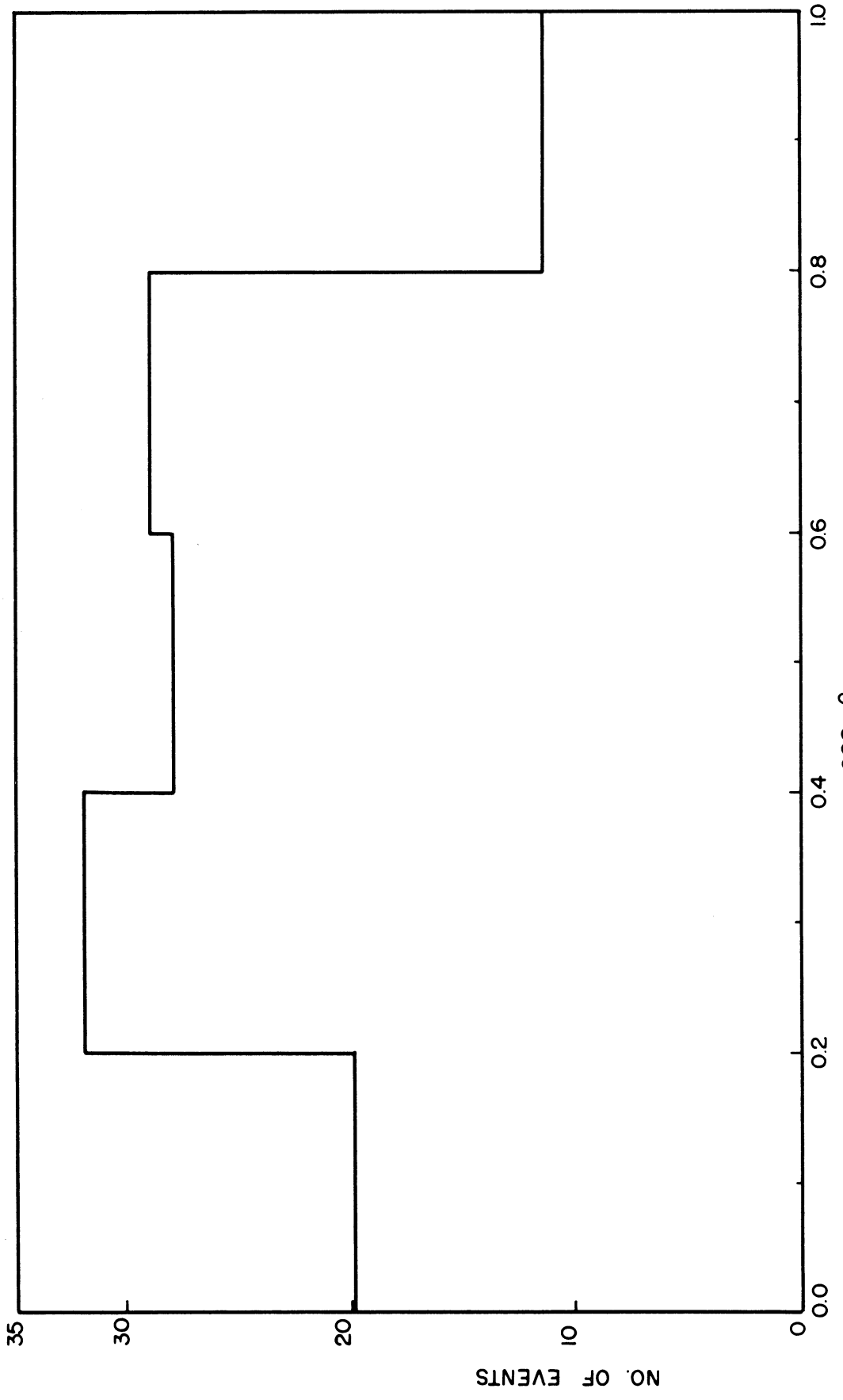

FIGURE 14 Experimental Cos θ Distribution of 118 Unambiguous Events

the relative probability of $F_J(\epsilon, x)$ to $F_{J'}(\epsilon, x)$ is

$$P_J^{J'} = \frac{\prod_{i=1}^{N} F_{J'}(\epsilon_i, x_i)}{\prod_{i=1}^{N} F_J(\epsilon_i, x_i)} \qquad (4\text{-}1)$$

Now, as an example, suppose that there is some region on the (ϵ, x) surface where $F_{J'} \ll F_J$. That is, in this region, by hypothesis J' there should be few events while by hypothesis J there should be a large number of events. It follows then that $P_J^{J'}$ can become a very small number if a large number of events occur in this region of the (ϵ, x) surface. Similarly if few events occur in this region but many occur in a region where $F_{J'} \gg F_J$ the quantity $P_J^{J'}$ can become very large. Thus one would tend to accept hypothesis J is $P_J^{J'}$ were less than 1 and reject it if $P_J^{J'}$ were greater than 1. This type of statistical test therefore has the advantage that it provides a shape dependent comparison of the data with two alternative hypotheses. It has the disadvantage that it can be extremely sensitive to a single point of the data. This latter remark is of special importance in the present investigation. It must be recalled that the distribution functions $F_J(\epsilon, x)$ are obtained by an approximation which discards higher order terms. Thus the existence of one event which has zero probability on the basis of a given distribution function does not necessarily rule out the possibility of the distribution function being the true one. It should be pointed out further that the existence of experimental error in the quantities ϵ and x prevents the assignment of the value

zero of $F_J(\epsilon, x)$. In the calculation of P_{0-}^{2+} and P_{0-}^{1-} from the data obtained in this experiment there were three instances in which $F_{JP}(\epsilon_i, x_i)$ could have been zero had not the existence of experimental error been recognized. The procedure adopted was to use an $F_{JP}(\epsilon_i, x_i)$ calculated assuming ϵ_i and x_i to have the maximum experimental error. In the case where there exist more than two possible distribution functions the most nearly correct distribution function will, in a large sample, be the one which consistently has a high probability relative to all the others.

Before proceeding it should be remarked that in the actual computation of the relative probability exceedingly large numbers are encountered. Thus it becomes convenient to consider the logarithm of relative probability, which is

$$\log P_J^{J'} = \sum_{i=1}^{N} \log \frac{F_{J'}(\epsilon_i, x_i)}{F_J(\epsilon_i, x_i)}$$

The mean value of this quantity is then

$$\overline{\left(\log \frac{F_{J'}}{F_J}\right)}_{\text{expt.}} = \frac{1}{N}\left(\sum_{i=1}^{N} \log \frac{F_{J'}(\epsilon_i, x_i)}{F_J(\epsilon_i, x_i)}\right)$$

As a means of comparison between the theory and the experimental data is is useful to calculate the expected values of the mean $\log \frac{F_{J'}}{F_J}$ assuming ϵ and x to be distributed according to the various proposed distribution functions. For example, the expected value of the mean $\log \frac{F_{J'}}{F_J}$ if F_J is assumed to be the correct distribution function is

$$\left\langle \log \frac{F_{J'}}{F_J} \right\rangle_{F_J} = \int\int \left[\log \frac{F_{J'}(\epsilon, x)}{F_J(\epsilon, x)} \right] F_J(\epsilon, x) d\epsilon dx. \qquad (4\text{-}2)$$

As a measure of dispersion about the expected value of the mean it is necessary to calculate the theoretical second moment. This is

$$\mu^{(2)}_{F_J} = \left\{ \left\langle \log^2 \frac{F_{J'}}{F_J} \right\rangle_{F_J} - \left\langle \log \frac{F_{J'}}{F_J} \right\rangle^2 \right\} \qquad (4\text{-}3)$$

where

$$\left\langle \log^2 \frac{F_{J'}}{F_J} \right\rangle_{F_J} = \int\int \left[\log \frac{F_{J'}(\epsilon, x)}{F_J(\epsilon, x)} \right]^2 F_J(\epsilon, x) d\epsilon dx.$$

The theoretical standard deviation is perhaps the more familiar quantity and this is defined as the square root of the second moment. Then if F_J is the correct distribution function it is highly probable that the experimental result will lie within several standard deviations of the expected value. It is clear that if both $\left(\log \frac{F_{J'}}{F_J}\right)_{\text{expt.}}$ and the theoretical quantities defined in equations (4-2) and (4-3) are multiplied by the factor N then the experimental and theoretical quantities can still be compared. As a matter of convenience and also in an attempt to follow conventions established by previous authors this will be done here. Then the expected values of the mean and the second moment become

$$\left(\log P_J^{J'}\right)_{F_J} = N \left\langle \log \frac{F_{J'}}{F_J} \right\rangle_{F_J}$$

and

$$\sigma^2_{F_J} = N\mu^{(2)}_{F_J} ,$$

respectively. The expectation values and their standard deviations h have been calculated using the parity conserving distribution functions. The results are listed in Table VII, and these values will be compared with the experimental results.

TABLE VII

Expected Values of Probability Ratios

Probability Ratio	As a Function of N	For N = 136
$\left\langle P^{1+}_{0-}\right\rangle_{F_{0-}}$	$10^{-0.085N \pm 0.32\sqrt{N}}$	$10^{-11.7 \pm 3.8}$
$\left\langle P^{1+}_{0-}\right\rangle_{F_{1+}}$	$10^{+0.059N \pm 0.20\sqrt{N}}$	$10^{8.3 \pm 2.3}$
$\left\langle P^{1-}_{0-}\right\rangle_{F_{0-}}$	$10^{-0.39N \pm 0.51\sqrt{N}}$	$10^{-53.0 \pm 5.8}$
$\left\langle P^{1-}_{0-}\right\rangle_{F_{1-}}$	$10^{+0.98N \pm 2.53\sqrt{N}}$	$10^{+133.0 \pm 29.6}$
$\left\langle P^{2+}_{0-}\right\rangle_{F_{0-}}$	$10^{-0.36N \pm 1.13\sqrt{N}}$	$10^{-49.0 \pm 13.2}$
$\left\langle P^{2+}_{0-}\right\rangle_{F_{2+}}$	$10^{+0.29N \pm 0.68\sqrt{N}}$	$10^{+39.4 \pm 8.0}$

- - - - - -

It is also necessary to introduce some quantitative measure of the degree of deviation of the experimental results from a given theoretical distribution function. In the limit of large N the deviation of the data from the correct distribution function will be Gaussian distributed. The well-known χ^2 test[31] is then applicable. In this test

the quantity

$$M = \sum_{i=1}^{r} \frac{(f_i - Np_i)}{Np_i} \qquad (4\text{-}4)$$

is χ^2 distributed with r-1 degrees of freedom. Here Np_i is the expected number of events in the i^{th} interval and f_i is the number of events in this interval which actually occur in the data. The χ^2 distribution will then give the probability that this or a larger value of M arise from N random events distributed according to a particular distribution function. It is important to realize that the χ^2 test cannot distinguish between two distribution functions which predict the same values of Np_i for every interval. The χ^2 test suffers from a disadvantage similar to that of the relative probabilities test. That is, a large deviation from the expected value in one interval, which could be the result of experimental error, can lead to a very low χ^2 probability.

In the previous section it was mentioned that the data contained 18 decays in which one of the π^+ mesons and the π^- meson leave the chamber before they come to rest. Thus it is not possible to identify the π^- meson. Kinematically, however, these events are completely specified so that the π^- energy is known to be one of the two escaping pion energies. The existence of this situation introduces a certain amount of bias into the data, and therefore it is necessary to adopt a consistent method of evaluating this bias. The method which has been adopted is to first calculate all possible relative probabilities, $P_{JP}^{J'P'}$. Among these numbers one distribution

function will have the highest relative probability. In this case it is the distribution function for the 0- spin-parity combination. The relative probabilities are then written in the form P^{JP}_{0-} and now they will be seen to all have values between 0 and 1. Now the effect of the 18 ambiguous events can be estimated by computing the relative probability for the two possible choices of the π^- energy. Of these two possibilities the one which tends to make the relative probability larger, that is, least favorable to 0-, is then multiplied by the value of the relative probability which was obtained for the first 118 events. This procedure carried out 18 times. If at any time the relative probability P^{JP}_{0-} approaches closely the expected value $\left\langle P^{JP}_{0-} \right\rangle_{F_{JP}}$ obtained by assuming F_{JP} to be the correct distribution function then the data is also consistent with the JP hypothesis. It should be noted that, for the statistical procedures chosen, this is the most severe assignment of the ambiguous events that could be made. It will be shown below that, except for 2-, in no case does the data appear consistent with any spin-parity combination other than 0-.

The relative probabilities for the 118 unambiguous events are

$$P^{1+}_{0-} = 10^{-14.9},$$

$$P^{1-}_{0-} = 10^{-27.7},$$

and

$$P^{2+}_{0-} = 10^{-10.2}.$$

If the 18 ambiguous events are then distributed in favor of the 1+ spin-parity combination the resulting relative probability is

$$(P^{1+}_{0-})_{\text{corr. } 1+} = 10^{-11.9} \quad .$$

This is 8.8 standard deviations from the expected value $\left\langle P^{1+}_{0-} \right\rangle_{F_{1+}}$ while it is within one standard deviation of $\left\langle P^{1+}_{0-} \right\rangle_{F_{0-}}$. For the 1-distribution the largest value of the relative probability which can be obtained is

$$(P^{1-}_{0-})_{\text{corr. } 1-} = 10^{-23.3}$$

which is 5.5 standard deviations from $\left\langle P^{1-}_{0-} \right\rangle_{F_{1-}}$ and 5.0 standard deviations from $\left\langle P^{1-}_{0-} \right\rangle_{F_{0-}}$. Similarly, for the 2+ case the corrected relative probability is

$$(P^{2+}_{0-})_{\text{corr. } 2+} = 10^{-8.2} \quad .$$

This result is 6.0 standard deviations from the expected value for F_{2+} and 3.1 from that for F_{0-}. Thus even when the 18 ambiguous events are allowed to assume values of ϵ and x which make the various relative probabilities least favorable for 0- the data cannot be made to be consistent with any one of the distribution functions for other spin-parity combinations. Furthermore, and this is perhaps the most important result, the relative probabilities obtained by this procedure are not inconsistent with the 0- distribution function.

The next step in the analysis is the testing of the experimental data for consistency with the 0- distribution. To do this the value of ϵ and cos θ for the 18 ambiguous events are distributed in accordance with the probabilities obtained from the 0- distribution function. The procedure is to divide the energy or angular range into a definite number of equal intervals and then to calculate the probabilities for each of

these intervals. That is, the area under the curve representing the appropriate spectrum is computed. The events are then distributed with respect to the weights given by the probabilities concerned. For example, if a certain interval was twice as probable as another and there were three uncertain events which could fall in either of the two intervals then the events would be distributed with two to the most probable and one to the least probable interval. This procedure must, of course, be done separately for the ϵ and cos θ distribution. When the values of ϵ for the uncertain events are distributed according to F_{0-} and added to the other 118 events an energy spectrum results which is shown in Figure 15. The relative probabilities calculated for this spectrum are

$$(P^{1+}_{0-})_{\substack{\text{corr. } 0- \\ (\epsilon)}} = 10^{-13.03}$$

$$(P^{1-}_{0-})_{\substack{\text{corr. } 0- \\ (\epsilon)}} = 10^{-27.50},$$

and

$$(P^{2+}_{0-})_{\substack{\text{corr. } 0- \\ (\epsilon)}} = 10^{-10.88} \quad .$$

Here, the relative probability for 1+ is within one standard deviation of $\left\langle P^{1+}_{0-} \right\rangle_{0-}$ while $(P^{1-}_{0-})_{\text{corr. } 0-}$ and $(P^{2+}_{0-})_{\text{corr. } 0-}$ are 4.4 and 2.8 standard deviations from $\left\langle P^{1-}_{0-} \right\rangle_{0-}$ and $\left\langle P^{2+}_{0-} \right\rangle_{0-}$ respectively. The χ^2 test of this distribution yields a value of M with a 25% probability. When the cos θ distribution is treated in the same way one obtains

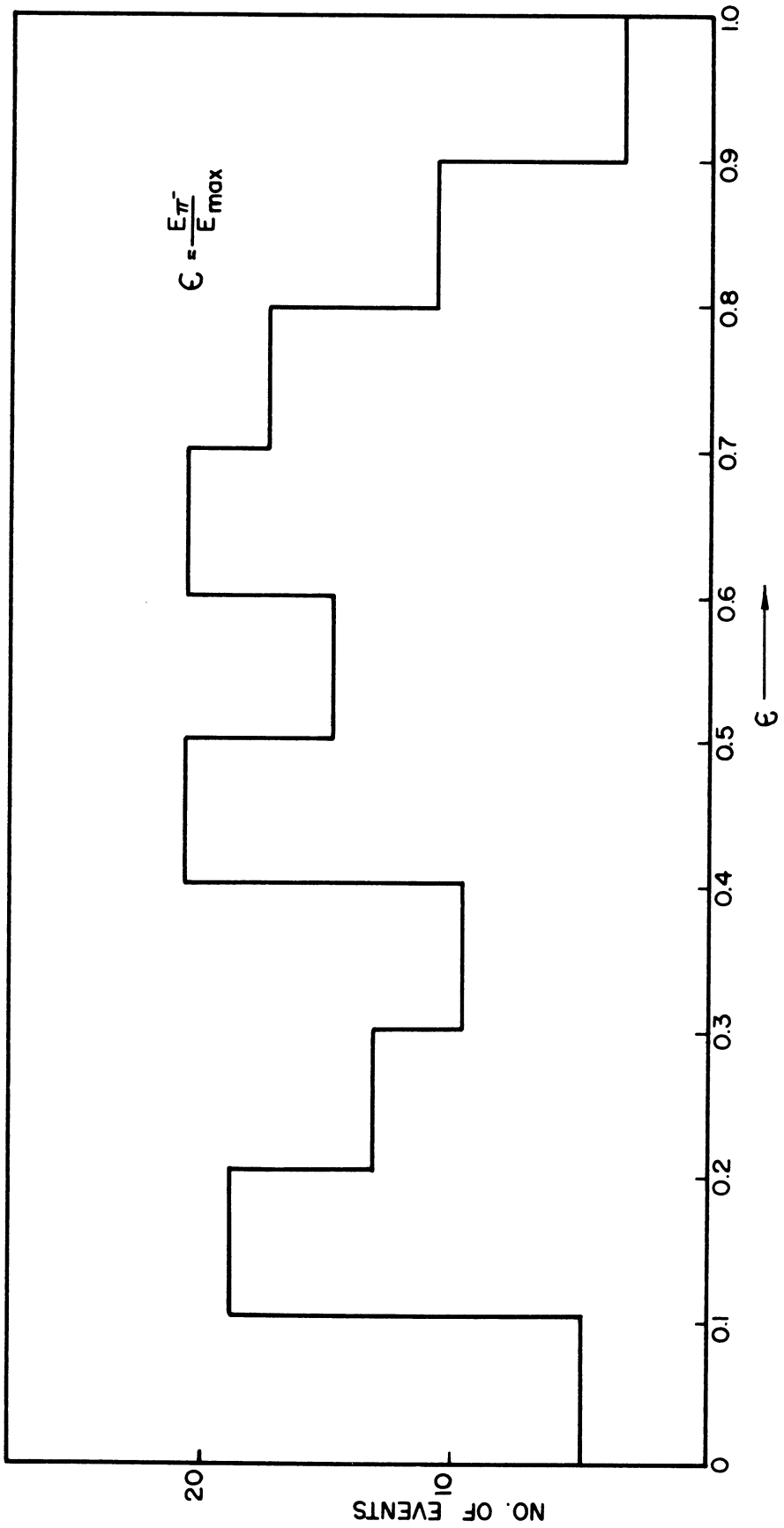

FIGURE 15 Experimental Energy Distribution Corrected According To F_o-

$$(P^{1+}_{0-})_{\substack{\text{corr. } 0- \\ (\cos\theta)}} = 10^{-13.20} ,$$

$$(P^{1-}_{0-})_{\substack{\text{corr. } 0- \\ (\cos\theta)}} = 10^{-25.90} ,$$

and

$$(P^{2+}_{0-})_{\substack{\text{corr. } 0- \\ (\cos\theta)}} = 10^{-12.64} .$$

Where $(P^{1+}_{0-})_{\substack{\text{corr. } 0- \\ (\cos\theta)}}$ is again within one standard deviation of $\langle P^{1+}_{0-} \rangle_{0-}$ and $(P^{1-}_{0-})_{\substack{\text{corr. } 0- \\ (\cos\theta)}}$ and $(P^{2+}_{0-})_{\substack{\text{corr. } 0- \\ (\cos\theta)}}$ are 4.7 and 2.9 standard deviations from $\langle P^{1-}_{0-} \rangle_{0-}$ and $\langle P^{2+}_{0-} \rangle_{0-}$, respectively. This spectrum is plotted in Figure 16. The χ^2 probability for the cos θ distribution is 7%. It should be noted that this quantity is largely influenced by the interval from 0.8 to 1.0. If this interval is excluded a probability of 25% is obtained.

It is of interest to consider the best and worst values of the χ^2 probability which can be obtained by arrangement of the uncertain portion of the data. For the energy distribution one can obtain a χ^2 probability as high as 40% and as low as 7%. For the cos θ distribution the highest probability is 20% and the lowest is 2%.

The final test which shall be considered is one which was proposed recently by Orear.[32] Orear has pointed out that the low energy end of the τ^+ decay spectrum for spin zero is independent of the momentum while that for spin 1 has at least a p^2 dependence. This can be seen by reference to equation (2-25). He assumes that the distribution functions

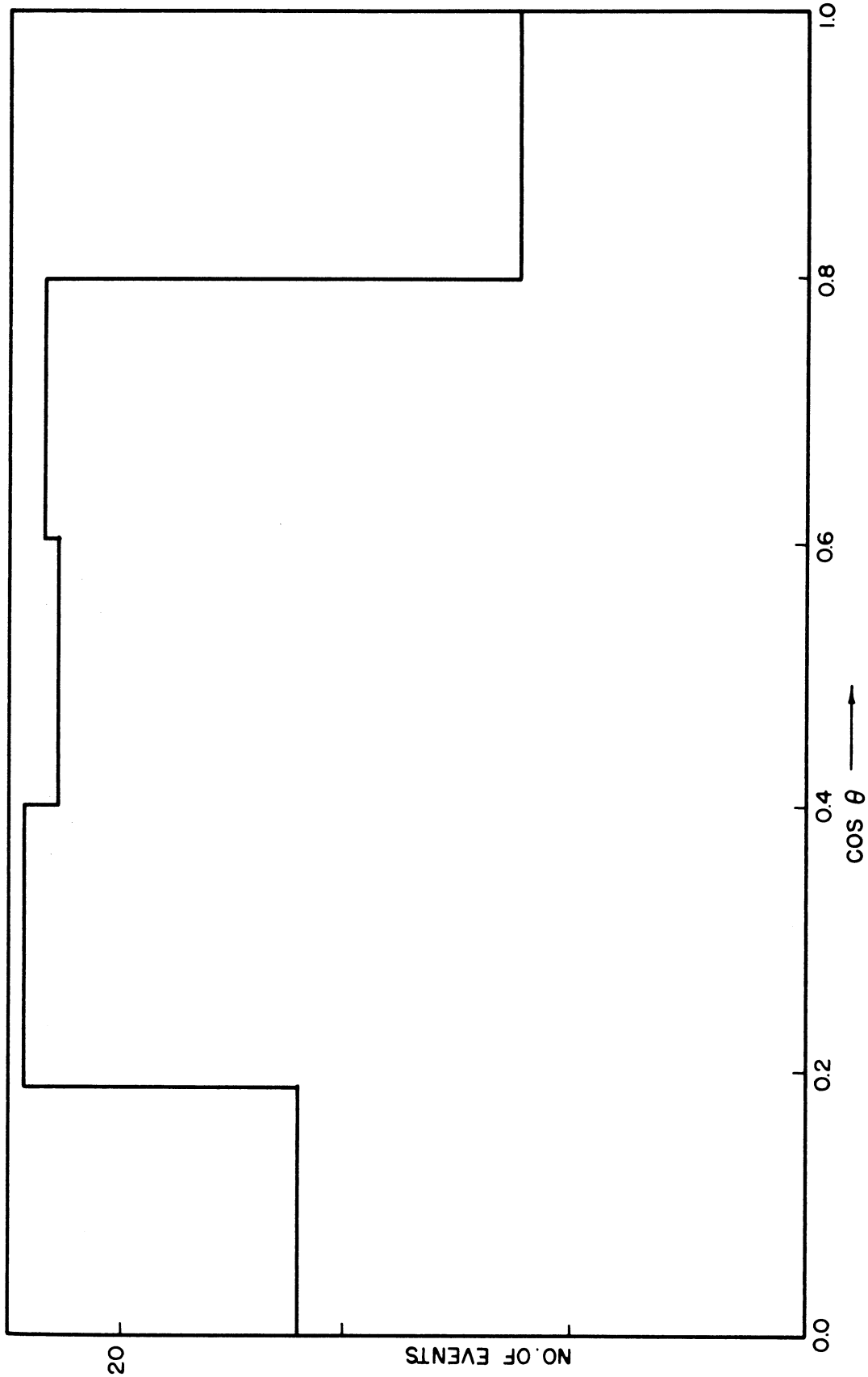

FIGURE 16 Experimental Cos θ Distribution Corrected According To F_{0-}

for spin 1 and spin zero are identical for values of the π^- energy above 10 Mev. Below 10 Mev the distribution functions are normalized according to

$$\int_{0.0}^{0.2} f_0(\epsilon)\rho(\epsilon)\,d\epsilon = \int_{0.0}^{0.2} f_1(\epsilon)\rho(\epsilon)\,d\epsilon \qquad (4\text{-}5)$$

where $\rho(\epsilon)$ is the density in phase space. This test still rests heavily on the original assumptions of the Dalitz-Fabri mode. First, the assumption of the validity of the conservation of angular momentum is, of course, not relaxed. Secondly the assumption that the higher powers of the momentum occurring in the distribution function do not contribute still must be included. If the second assumption is correct then the test is to a certain extent independent of whether or not parity is conserved in the decay. This follows from the fact that the 1- term has at least a dependence on the fourth power of the momentum, and thus even though a mixing of the two parity states did occur in the decay the contribution from the state of negative parity would be negligible. This is the reson that the factor $\rho(\epsilon)$ is the same on both sides of the equation. The test proposed by Orear then consists of calculating the relative probabilities P_0^1 for only these low energy pions. The reason for the sensitivity of this test in distinguishing between spins 1 and 0 lies in the marked difference in the shape of the two energy spectra in this region. Thus the quantity

$$P_0^1 = \frac{\prod_{i=1}^{24} f_1(\epsilon_i)}{\prod_{i=1}^{24} f_0(\epsilon_i)}$$

has been calculated using the data obtained in this experiment. The result is

$$P_0^1 = 10^{-1.9} ,$$

that is, the relative probability is in favor of spin zero.

4.3 Resume of Results

The results of the analysis carried out in the previous section indicate that the data is inconsistent with spin-parity combinations 1+, 1-, and 2+. The 2- spectrum cannot be determined since it depends on the values of certain constants which are not known. With this exception the data indicate that if the spin of the τ^+ is less than or equal to 2 then it probably has zero spin. The experimental value of P_{0-}^{1-} gives the least agreement with theoretical prediction on the 0- hypothesis but in no way is it possible to arrange the uncertain portion of the data such that the results which would be expected if 1- were the correct spin-parity combination are obtained. The value of P_{0-}^{2+} is in fair agreement with the predicted number, and the results for P_{0-}^{1+} are excellent. If parity is not conserved in the decay then the results are inconsistent with spin 1 for the τ^+ meson but are consistent with spin 0. There appears to be, at present, no means of testing for consistency with spin 2 if parity is not conserved.

Comparison of the data obtained in this experiment with the emulsion data[13,17] reveals no striking differences in the data obtained

by the two experimental techniques. In particular, the number of low energy pions found in this experiment is roughly the same per cent of the total sample as that found in some of the more recent emulsion experiments.[32] This tends to confirm the argument that the absence of low energy π^- events in earlier experiments was due to bias of some sort.[33] Also, the relative probabilities calculated from the data in this experiment have about the same amount of agreement with expected values as those obtained from the emulsion data. Thus the important result of this experiment appears to be that it confirms, within the limits of experimental accuracy, the results of the emulsion experiments.

BIBLIOGRAPHY

1. Brown, R., U. Camerini, P. H. Fowler, H. Muirhead, C. F. Powell, and D. M. Ritson, 1949, Nature, Lond., 163, 82.

2. T. D. Lee and J. Orear, Phys. Rev. 100, 932 (1955).

3. S. B. Treiman and H. W. Wyld, Jr., Phys. Rev. 99, 1039 (1955).

4. S. Goldhaber, Proceedings of the Sixth Annual Rochester Conference on High Energy Physics, (Interscience Publishers Inc., New York, 1956) p. V-25.

5. V. Fitch and R. Motley, Phys. Rev. 101, 496 (1956).

6. V. Fitch and R. Motley, Phys. Rev. 105, 265 (1957).

7. L. Alvarez and S. Goldhaber, Nuovo Cimento 2, 344 (1955)

8. G. Harris, J. Orear, and S. Taylor, Phys. Rev. 100, 932 (1955).

9. T. F. Hoang, M. F. Kaplon, and G. Yekutielli, Phys. Rev. 105, 278 (1957).

10. J. L. Brown, D. A. Glaser, and M. L. Perl, Phys. Rev. (To be published).

11. K. Lande, L. M. Lederman and W. Chinowski, Phys. Rev. 105, 1925 (1957).

12. F. Eisler et al. (To be published).

13. Gottstein, K., Proceedings of the Sixth Annual Rochester Conference on High Energy Physics, (Interscience Publishers, Inc., New York, 1956), p. V-9.

14. Dalitz, R., Phil. Mag. 44, 1068 (1953).

15. Dalitz, R., Phys. Rev. 94, 1046 (1954).

16. Fabri, E., Nuovo Cimento XI, 479 (1954).

17. M. Baldo-Ceolin, A. Bonnetti, W. D. B. Greening, S. Limentani, M. Merlin, G. Vanderhaege, Nuovo Cimento (To be published).

18. T. D. Lee and C. N. Yang, Phys. Rev. 104, 254 (1956).

19. Wu, C. S., Ambler, E., Haywood, R. W., Hoppes, D. D., Hudson, R. P. Phys. Rev. 105, 1413 (1957).

20. Wu, C. S., Ambler, E., Haywood, R. W., Hoppes, D. D., Hudson, R. P. Phys. Rev. 106, 1363 (1957).

21. Garwin, R. L., Lederman, L. M., and Weinrich, M., Phys. Rev. 105, 1415 (1957).

22. E. Lomon, Proceedings of the Seventh Annual Rochester Conference on High Energy Physics, 1957 (Interscience Publishers, Inc., New York, 1957), Session VIII.

23. R. M. Sternheimer, R.S.I. 24, 573, (1953).

24. D. C. Rahm, Ph.D. Thesis, University of Michigan, 1956 (Unpublished).

25. Glaser, Rahm and Dodd, Phys. Rev., 102, 1653 (1956).

26. D. I. Meyer, M. L. Perl and D. A. Glaser, Phys. Rev. 107, 279 (1957).

27. T. F. Hoang, (To be published).

28. C. Graves, Unpublished Report, Michigan Bubble Chamber Group (1956).

29. R. Marshak, Meson Physics, McGraw Hill, 1952, Chapter 5.

30. P. Ammiraju and L. M. Lederman, Nuovo Cimento IV 283 (1956).

31. H. Cramer, The Elements of Probability Theory, John Wiley, New York (1955).

32. J. Orear, Phys. Rev. 106, 834 (1957).

33. Orear, Harris and Taylor, Phys. Rev. 102, 1676 (1956).

APPENDIX

List of the Data

Frame No.	ϵ	ϵ_1	ϵ_2	cos θ
39316	0.77	0.54	0.20	0.48
39881	0.60	0.83	0.08	0.88
41772	0.26	0.75	0.49	0.34
42041	0.20	0.89	0.41	0.70'
42047	0.15	0.90	0.44	0.75
42064	0.68	0.68	0.14	0.66
42112	0.68	0.65	0.18	0.57
42526	0.86	0.52	0.12	0.66
42668	0.49	0.52	0.50	0.02
42734	0.40	0.83	0.28	0.65
42894	0.41	0.67	0.45	0.27
42911	0.89	0.49	0.15	0.63
42963	0.06	0.72	0.72	0.00
43209	0.75	0.75	0.00	0.98
43262	0.14	0.75	0.65	0.26
43305	0.61	0.81	0.08	0.86
43671	0.21	0.86	0.48	0.54
44012	0.70	0.41	0.38	0.02
44091	0.74	0.59	0.16	0.57
44191	0.36	0.64	0.48	0.19
44855	0.24	0.79	0.48	0.43

List of the Data Cont'd

Frame No.	ϵ	ϵ_1	ϵ_2	cos θ
44954	0.07	0.76	0.68	0.19
45028	0.45	0.78	0.27	0.58
45792	0.44	0.68	0.38	0.58
45862	0.46	0.78	0.26	0.60
46120	0.13	0.84	0.53	0.53
46196	0.85	0.47	0.17	0.47
46260	0.20	0.75	0.54	0.30
46429	0.28	0.74	0.46	0.36
46544	0.73	0.73	0.03	0.91
46585	0.92	0.31	0.27	0.07
46875	0.40	0.69	0.40	0.35
46966	0.17	0.91	0.41	0.76
47149	0.50	0.62	0.38	0.28
47416	0.12	0.72	0.65	0.12
47422	0.88	0.32	0.30	0.03
47904	0.81	0.47	0.24	0.33
48579	0.16	0.68	0.67	0.03
48624	0.41	0.87	0.22	0.78
48996	0.21	0.76	0.53	0.32
49143	0.08	0.80	0.61	0.41
49313	0.13	0.79	0.57	0.38
49419	0.69	0.68	0.13	0.70
49647	0.14	0.81	0.54	0.46

List of the Data Cont'd

Frame No.	ϵ	ϵ_1	ϵ_2	cos θ
49873	0.12	0.85	0.57	0.48
49893	0.45	0.68	0.36	0.36
50017	0.71	0.60	0.28	0.40
50304	0.75	0.75	0.00	1.00
50511	0.17	0.72	0.62	0.16
50582	0.75	0.75	0.00	1.00
50737	0.61	0.79	0.10	0.81
50798	0.14	0.79	0.58	0.34
51125	0.56	0.62	0.31	0.36
51194	0.48	0.85	0.17	0.78
51453	0.71	0.80	0.09	0.89
51565	0.68	0.70	0.13	0.70
52390	0.84	0.44	0.22	0.36
52596	0.41	0.80	0.28	0.61
52896	0.53	0.58	0.38	0.24
53176	0.66	0.68	0.15	0.66
53181	0.69	0.60	0.22	0.48
53272	0.66	0.47	0.36	0.13
53297	0.34	0.87	0.27	0.74
53369	0.30	0.90	0.31	0.74
55275	0.64	0.62	0.56	0.07
55436	0.76	0.41	0.33	0.12
55526	0.11	0.79	0.63	0.29

List of the Data Cont'd

Frame No.	ϵ	ϵ_1	ϵ_2	cos θ
55637	0.50	0.83	0.16	0.78
56189	0.71	0.47	0.32	0.18
56386	0.26	0.84	0.44	0.52
56412	0.66	0.65	0.19	0.57
56569	0.68	0.59	0.23	0.45
56670	0.32	0.67	0.50	0.21
56700	0.67	0.57	0.26	0.36
56978	0.21	0.73	0.55	0.24
57042	0.26	0.71	0.52	0.25
57204	0.31	0.87	0.33	0.67
57428	0.52	0.75	0.23	0.60
57486	0.13	0.74	0.63	0.18
57516	0.18	0.78	0.52	0.38
57839	0.15	0.92	0.40	0.83
57880	0.46	0.74	0.31	0.50
58102	0.48	0.64	0.38	0.30
58435	0.38	0.82	0.33	0.57
58592	0.46	0.72	0.34	0.44
58819	0.11	0.88	0.51	0.66
58851	0.81	0.56	0.12	0.64
59180	0.47	0.76	0.26	0.58
59326	0.32	0.71	0.45	0.32
59499	0.13	0.91	0.49	0.73

List of the Data Cont'd

Frame No.	ϵ	ϵ_1	ϵ_2	cos θ
59591	0.51	0.63	0.36	0.32
59677	0.43	0.65	0.41	0.28
60128	0.48	0.63	0.43	0.24
60169	0.12	0.71	0.67	0.06
60288	0.07	0.78	0.66	0.26
60549	0.57	0.74	0.19	0.58
60610	0.21	0.75	0.54	0.29
60683	0.26	0.72	0.52	0.27
60691	0.84	0.49	0.17	0.50
60770	0.85	0.52	0.15	0.58
60799	0.24	0.92	0.35	0.77
60848	0.93	0.44	0.14	0.65
60937	0.06	0.81	0.62	0.46
61492	0.56	0.74	0.21	0.62
61549	0.69	0.69	0.09	0.76
61922	0.44	0.68	0.36	0.36
62015	0.14	0.89	0.47	0.69
62053	0.50	0.76	0.23	0.62
62343	0.49	0.70	0.22	0.56
62737	0.64	0.48	0.38	0.13
63457	0.90	0.30	0.30	0.00
52335	0.74	0.74	0.02	0.96
53270	0.64	0.64	0.25	0.45

List of the Data Cont'd

Frame No.	ϵ	ϵ_1	ϵ_2	cos θ
56369	0.58	0.58	0.33	0.31
56457	0.53	0.53	0.44	0.33
59615	0.63	0.63	0.23	0.48
63421	0.71	0.71	0.08	0.81

Data for the 18 Ambiguous Events

Frame No.	ϵ_A	ϵ_B	$\epsilon_{Stopping}$	cos θ_A	cos θ_B
41856	0.54	0.78	0.15	0.72	0.54
43245	0.70	0.65	0.13	0.65	0.69
43564	0.45	0.71	0.33	0.44	0.17
44194	0.80	0.24	0.45	0.30	0.47
47263	0.86	0.31	0.31	0.00	0.69
48442	0.76	0.53	0.23	0.39	0.61
50297	0.84	0.50	0.15	0.54	0.74
50562	0.63	0.56	0.37	0.23	0.30
53308	0.56	0.75	0.16	0.68	0.54
57100	0.72	0.59	0.19	0.51	0.63
59673	0.76	0.61	0.13	0.65	0.87
60543	0.39	0.62	0.50	0.14	0.12
60997	0.47	0.81	0.21	0.70	0.39
62065	0.55	0.70	0.22	0.58	0.42
44389	0.90	0.36	0.24	0.23	0.80
49261	0.77	0.69	0.07	0.78	0.89
51531	0.74	0.55	0.22	0.43	0.60
52908	0.65	0.47	0.34	0.17	0.36